Microfluidic Platform for Multi-parameter Analysis of Live Single Cells

by

Meryl Rodrigues

A Thesis Presented in Partial Fulfillment
of the Requirements for the Degree
Master of Science

Approved November 2014 by the
Graduate Supervisory Committee:

Deirdre R. Meldrum, Chair
Laimonas Kelbauskas
Jeffrey LaBelle

ARIZONA STATE UNIVERSITY

December 2014

ABSTRACT

Cellular heterogeneity is a key factor in various cellular processes as well as in disease development, especially associated with immune response and cancer progression. Cell-to-cell variability is considered to be one of the major obstacles in early detection and successful treatment of cancer. Most present technologies are based on bulk cell analysis, which averages the results acquired from a group of cells and hence misses important information about individual cells and their behavior. Understanding the cellular behavior at the single-cell level can help in obtaining a complete profile of the cell and a more in-depth knowledge of cellular processes. For example, measuring transmembrane fluxes oxygen can provide a direct readout of the cell metabolism.

The goal of this thesis is to design, optimize and implement a device that can measure the oxygen consumption rate (OCR) of live single cells. A microfluidic device has been designed with the ability to rapidly seal and unseal microchambers containing individual cells and an extracellular optical oxygen sensor for measuring the OCR of live single cells. The device consists of two parts, one chip with the sensor in microwells (top half, "sensor chip") and the other chip with channels and cells trapped in Pachinko-type micro-traps (bottom half, "cell chip"). When the two parts of the device are placed together the wells enclose each cell. Oil is flown in through the channels of the device to produce an isolated and sealed microchamber around each cell. Different fluids can be flowed in and out of the device, alternating with oil, to rapidly switch between a sealed and unsealed microenvironment around each cell. A fluorescent ratiometric dual pH and oxygen sensor is placed in each well of the sensor chip. The thesis focuses on measuring changes in the

oxygen consumption rate of each cell within a trap. Live and dead cells are identified using a fluorescent live/dead cell assay. Finally, the technology is designed to be scalable for high-throughput applications by controlling the flow rate of the system and increasing the cell array density.

DEDICATION

I dedicate this thesis to my parents Elizabeth Rodrigues and Michael Rodrigues along with my little sister Elfrida Rodrigues, without whom I would have never been who I am and where I am today. I would also like to dedicate this to all my friends who have constantly guided and supported me through everything I have ever done in my life.

TABLE OF CONTENTS

Page

CHAPTER Page

CHAPTER Page

LIST OF TABLES

Table Page

LIST OF FIGURES

Figure Page

Figure Page

Figure Page

1. INTRODUCTION

1.1 Cellular Heterogeneity

Cellular heterogeneity is common in eukaryotic cells and may lead to disease states (Lidstrom and Meldrum 2003). It plays a central role in disease development, including cancer metastasis (Sarkar et al. 2014). Cellular heterogeneity can arise in continuously changing cell microenvironments, rendering certain cells more fit in an entire cell population (Mannello & Ligi et al., 2012) by regulating their biochemical networks and regulatory enzymatic activities. Single cells can easily take advantage of the inherent random variability in gene expression to increase their survival at the expense of the rest of the clonal cell population helping them to survive and proliferate (Sarkar et al. 2014).

Cellular heterogeneity is observed in bacteria and protozoans during phenotypic switching due to antibiotic resistance or any other unfavorable microenvironmental condition. It is observed that this phenomenon is seen in embryonic development, immune response, and even cancer progression. Genetic mutations may not be the only reason that drives tumor progression and reoccurrence, but it is important along with small fractions of cancer cells having stem cell-like properties. These cells with self-renewal capacity may be the origin of tumor cell heterogeneity (Mannello & Ligi et al., 2012). "Heterogeneity is a documented natural occurrence in cancer cell population, and represents one of the major obstacles to the successful treatment of cancer."(Mannello & Ligi et al., 2012) It is therefore essential to understand the complexity of the cellular tissue microenvironment (Mannello & Ligi et al., 2012.).

1.2 The Need for Single Cell Analysis

The ability to monitor live cells is needed to understand cellular heterogeneity. A vast majority of current technologies rely on bulk cell analysis, thus providing average measurements of a cell population. The results do not provide the required knowledge for individual cells and their behavior. Knowledge of these underlying features can be a key to understanding various diseases like cancer and stroke (Ashili et al. 2011). The characterization of a tumor is typically based on bulk cell analysis, thus averaging the measurement for the molecular state present. In fact the region of diagnostic and/or therapeutic interest can be far smaller than the actual detection level. As a result, characterizing dominant clones from a single location in the tumor can tend to be misleading and end up in the use of the wrong therapies (Beckman, Schemmann, and Yeang 2012).

Ideally, single cell analysis measurements would include information about every analyte present in a cell and provide a complete profile of the cell that can be compared with other individual cells to get an in-depth knowledge of their behavior. This information would help in understanding the 'who makes what' i.e. the respective change caused in the system by every individual cell. In comparison to bulk cell analysis, single cell analysis can help to quantify which cell is causing what effect on the microenvironment or vice versa (Mannello & Ligi et al., 2012). Single cell analysis can also provide insights about interconnecting molecular events within a cell. These events can in turn provide information about the reason cellular heterogeneity exists. Every cell is different from another cell, even if it is from the same cell type (Lindström and

Andersson-Svahn 2010). Single cell analysis plays an important role in characterizing the physiopathological condition of these cells, right from oxygen consumption rate to gene expression. The knowledge gained from single cell analysis can have a great diagnostic, therapeutic, and prognostic value (Mannello & Ligi et al., 2012.).

1.3 Cell Targeting

1.3.1 Therapeutic Solutions

Pre-existing cellular heterogeneity and genetic variability give rise to the need for therapeutic solutions that consider cellular heterogeneity and its dynamics. "Genetic instability has been postulated to be the center to tumor evolution" (Beckman, Schemmann, and Yeang 2012). Analysis with single cell resolution can help in designing new drugs in addition to learning the behavior of existing drug responses in patients (Mannello & Ligi et al., 2012). Currently, drug therapies are directed to specific molecular states of cancerous cells. Present technologies use biomarkers for detecting different molecular states which are based on the stage of tumor, thus guiding the treatment strategy (Beckman, Schemmann, and Yeang 2012). Knowledge of the molecular profile of cells plays an important role in cancer research. This helps in the development of technologies for multi-parameter measurements of small clinical samples, which will help in developing more targeted and efficient therapies. Metabolic characteristics of single cancer cells can help in finding the origins, the stemness, and the "weak points" of these cells in terms of their eradication or reversion to their normal state. The information gleaned from single cell analysis can be the key to therapeutically

targeting every single cell in a tumor. The other thing that needs to be considered is the inherent heterogeneity in cancer cells along with the changing microenvironment due to tissue structures, thus making it a complex biological system (Mannello & Ligi et al., 2012).

1.3.2 Immune System

Single cell analysis can aid in understanding the function of the human immune system for diseased individuals. Single cells can provide information about the alterations seen in cellular behavior that occurs due to pathological conditions such as autoimmune diseases. In vitro measurements with single cell resolution (SCR) can be used to understand the cell reactivity of enzyme-linked immunospot assays (Mannello & Ligi et al., 2012).

1.3.3 Protein Analysis

There is a need for understanding the various biomolecular mechanisms of cellular processes, especially the proteins and proteinases since they provide information regarding the reason for cell differentiation which leads cells to pathophysiological and disease states. Single cell analysis enables measurement of protein profiles and cellular responses to internal and external stimuli, and provides information about cellular heterogeneity.

1.4 Existing Technologies for Single Cell Analysis

Recent improvements in sequencing technologies and molecular biology have led to the emergence of biomolecular quantitative analysis of single cells. Single cell RNA-

sequencing is another emerging technology being used to understand the expression-level variability in genetically identical cells (Geiler-Samerotte et al. 2013). It provides genome-wide information about gene expression levels, giving valuable insight into transcriptional heterogeneity in a cell population. There are several protocols for single-cell RNA-sequencing.

One study uses reverse transcription on cell lysates using oligo-dT primers where the cDNA is PCR amplified, fragmented and subjected to sample preparation for deep sequencing (Junker and van Oudenaarden 2014). Some of the difficulties faced in these techniques are the low detection efficiency of mRNA. However, with the use of microfluidics to reduce the reaction volume, detection efficiencies have increased (Junker and van Oudenaarden 2014).

Gene transcription plays an important role in cellular heterogeneity. A method to measure gene expression levels at the single cell level includes the DNA intercalating fluorescent dye SYBR green-based qPCR for quantitative analysis of gene expression in mammalian cells (Zeng et al. 2011). Other techniques use a single tube RT-qPCR approach in which cell lysis, cDNA synthesis by reverse transcriptase, and quantitative PCR are all performed in the same tube. These methods reduce the probability of mRNA loss but increase contamination during the process (Zeng et al. 2011). Single cell proteomics will need more advanced technologies to be developed to add a new dimension to the understanding of cell variability (Junker and van Oudenaarden 2014).

Phenotypic variability exists even when genetic and environmental differences in cells are minimized. Differences in phenotypes are observed in genetically similar cells. Flow cytometry is used on a large scale to understand and study phenotypic variability. Another technique known as High-Content Imaging (HCI) overcomes the issues faced with flow cytometry and helps to observe cellular phenotypes with a larger number of parameters. HCI allows simultaneous acquisition of many phenotypes along with automated data analysis resulting in information rich data sets (Geiler-Samerotte et al. 2013).

Several recent technologies concentrate on characterizing intercellular heterogeneity by analyzing single cells. Some of the analyses include methods to find transmembrane fluxes such as changes in pH and oxygen consumption rates, an indicator of cell metabolism, to provide information about the cellular microenvironment. A microenvironment deficient in oxygen, also known as hypoxia, is one of the main features in solid tumors. It is known that cells within a tumor do not have the same level of oxygenation. Such distinct changes along with pH changes within tumors are considered to be a key factor in disease onset and progression. In order to understand the effect of the physically changing microenvironment on the cell function, it is essential to have knowledge of the complete phenotype of the cell. This includes the characterization and quantification of oxygen consumption rates along with pH changes (Ashili et al. 2011). Oxygen consumption rate (OCR) is a critical parameter because it directly correlates with oxidative phosphorylation, the main process of ATP production within eukaryotic cells under adequate oxygen supply. Intracellular ATP levels reveal

mitochondrial activity and the amount of energy that is available for other metabolic processes like protein synthesis, cell division, and homeostasis. Small changes in the mitochondrial function are observed as an early response of cells that undergo apoptosis. Such changes are observed in conditions such as diabetes, aging, and cancer. Since ATP and metabolic processes play an important role in life and death decisions in these diseases, knowledge of the OCR can aid in understanding the response of these cells to different drug therapies (Molter et al. 2010).

A few technologies have been developed to measure OCR of single cells. The microrespirometer method is based on the determination of the cell oxygen consumption rate by placing the cell in a capillary next to an air bubble. The decrease in the size of the air bubble relates to the oxygen consumed by the cell (Piowland and Bernstein 1930). The main limitations of this approach are low throughput, measurement errors and lack of the desired resolution. Another technology uses electrochemical microsensor probes for detecting oxygen changes in a cell. The method measures the flux of molecular oxygen in the close proximity of single cells, thus measuring the changes in oxygen concentration due to corresponding physiological processes. The shortcomings of this technology are sensor drift, high detection limit, electrode fouling and difficulty in trying to place the sensor close to the single cell under observation (Molter et al. 2010). Nanosensor technology was developed to circumvent the problems arising due to cell-probe distance. In this method, fluorescent nanoprobes are self-assembled onto individual cells in a controlled manner to non-invasively measure the oxygen consumption rates in the proximity of these cells (Kuang and Walt 2007). Although the

system is high-throughput (~ 100 cells in parallel), it only measures oxygen fluxes. Also, the nanosensors may interfere with other cell processes and some cell types can even consume the sensor (Molter et al. 2010).

Recently, microwell arrays of various formats have become very popular as a tool for single cell analysis. They are being used for measuring physiological changes within cells. Array technology allows the use of multi-timepoint imaging and continuous monitoring experiments, which help in observing cellular dynamics over time. They also pose less stress to the cells in terms of electrophoretic, tethering or optical trapping strategies by reducing the physical, electrical, and optical forces used to trap or isolate single cells (Molter et al. 2010).

1.5 Microwell Based Technology for Measuring Oxygen Consumption Rates:

Current technologies concentrate on measuring oxygen consumption rates non-invasively by isolating single cells in microwells and monitoring the change in oxygen concentration around the cell using luminescent oxygen sensors. The cells residing in wells are first randomly seeded and the oxygen sensor is embedded in a ring on the circumference of the microwell. The sensor along with the cell is then sealed from the outside environment by using a glass lid to cover the top surface. The glass lid is brought down on the chip with the help of a piston that has a polydimethylsiloxane (PDMS) layer attached to it **(Figure 1.)**. The PDMS layer helps the glass lid to align with the microwells and achieve a proper seal. The oxygen consumption rate is derived from the oxygen sensor measurements using the phosphorescent properties of the

platinum porphyrin derived sensors using the optimized rapid lifetime determination (ORLD) method. This method measures the ratio of the two overlapping emission integration bins following an excitation pulse (Molter et al. 2009).

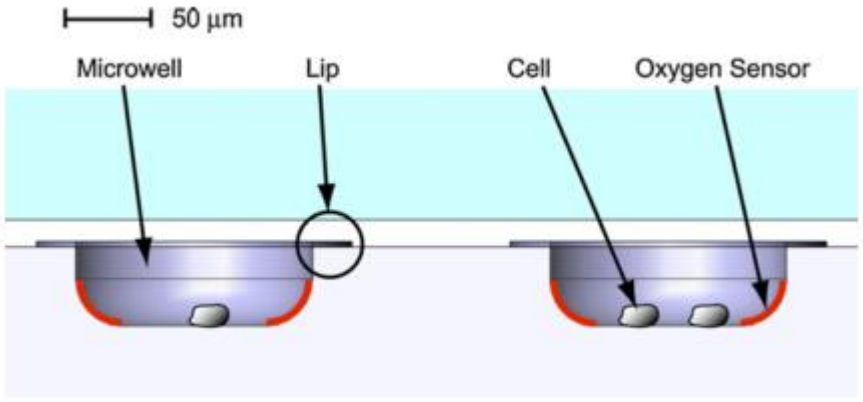

Figure 1: The Cells along with the Oxygen Sensor in the Microwells. They are Isolated from the Environment using a Glass Lid which is Pushed Down against the Lipped Wells using a Piston (Molter et al. 2009)**.**

The main shortcomings of this technology are:

- Cells are placed into wells using a random seeding method which can result in more than one cell in a microwell, thus reducing the efficiency of the array for single cell analyses. Data obtained from wells with multiple cells is an average of the number of cells in each well. The use of the piston on the top chip uses an external force generated by a 10 lb (4.5 kg) mass on the lips of the wells to achieve the seal. This force can damage the glass lid and/or the wells in the bottom chip.

- The close proximity of the cells with the sensors may influence the normal cell functionality because of photochemical activity of the sensor along with the reactivity of the oxygen species (Kelbauskas et al. 2012).

Another technology present in the Center for Biosignatures Discovery Automation (CBDA), in the Biodesign Institute follows the same principle as the system above with the exception that it uses two chips instead of one. The bottom chip has wells for the single cells and the top chip has wells with lips and sensors deposited in it **(Figure 2.)**. This method helps in eliminating the shortcoming that arises from the above technology due to the close proximity of the cell and sensor. The system also uses a cell loading microfluidic platform which aspirates and dispenses cells one at a time into each well (Kelbauskas et al. 2012). This enables the system to load only one cell in each well and eliminates the trapping of more than one cell. In the final setup, the chip with the sensor is brought down onto the chip with cells with the help of a piston. The two chips are sealed by applying weight (4-7 kgs) on top of the lid with the piston. Wells can also be unsealed by removing the weight and the glass lid (Kelbauskas et al. 2012).

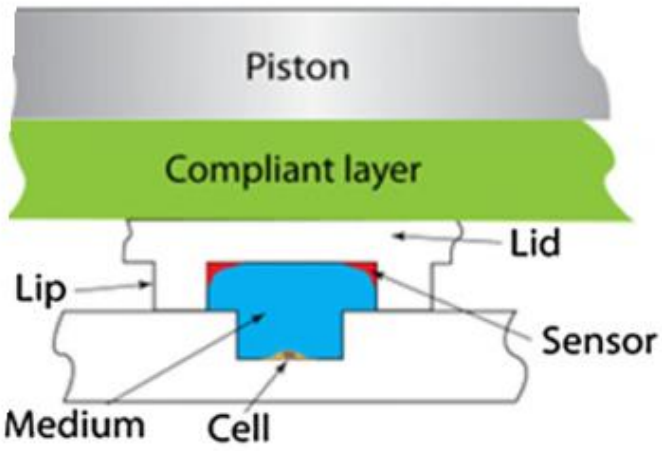

Figure 2: A System with the Sensor on the Top Lid (Chip) and the Cell in a Well in the Bottom Chip. The Two Chips are sealed by bringing the Lid (Top Chip) Down on the Bottom Chip with the use of a Piston (Kelbauskas et al. 2012)**.**

However, this technology has a few drawbacks:

- The time required to load cells into the wells increases as the number of wells increases, thus reducing efficiency.
- The weight required to achieve a seal between the two chips increases as the number of wells (well density) increases.

CHAPTER 2: DESIGN AND IMPLEMENTATION

2.1 Approach

This thesis strives to overcome the drawbacks of the technology described in Section 1.5 by developing a device that uses different liquids to seal and unseal the wells as opposed to the use of a glass lid and considerable amount of force. This approach uses a medium (e.g. mineral oil) with low permeability to oxygen as a sealing method to isolate single cells contained within microwells from the environment. The design consists of two chips, one of which has the sensor deposited into the wells (sensor chip) and the other which has microfluidic channels and traps for the cells (cell chip) **(Figure 3.)**. Once the two chips are brought together using a semi-automated assembling unit which has control in the x, y, and z axes. Using a manually controlled syringe, the system is then primed with medium which flows through the channels and enter into the wells with cells. Next, mineral oil is flown into the system where it only flows through the channels and does not enter the wells due to the wetting phenomenon between aqueous medium, oil and glass surface (Zettlemoyer, Aronson, and Lavelle 1970) creating a sealed environment around each cell. Oil having a low permeability to oxygen prevents air from entering the system thus sealing the environment of the cells trapped inside the wells (Figure 3).

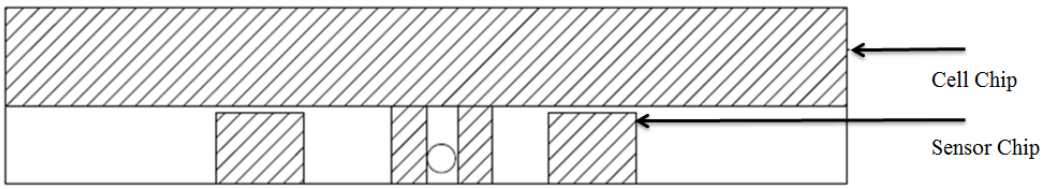

Figure 3: Cross section of the cell chip and the sensor chip.

2.1.1 Enabling Properties of Mineral Oil

Introducing mineral oil as a sealing medium eliminates the use of a glass substrate and force to seal the wells, which was seen in the previous methods. A few properties of mineral oil enable it to seal cells in wells, as explained in the next section.

2.1.1.1 Solubility of Oxygen in Mineral Oil

Mineral Oil is a non-polar liquid; that is, it contains bonds between atoms with similar electronegativity such as carbon-hydrogen bonds. Non-polar liquids do not have free charge. Oxygen on the other hand has a couple of unpaired, negatively-charged electrons. Due to the non-polarity of mineral oil, oxygen has a much lower diffusion coefficient in oil than in water. Due to the low diffusion rate of oxygen, mineral oil acts as a good sealing medium for oxygen from the atmosphere (Diepart et al. 2010).

2.1.1.2 Interfacial Tension

In a liquid, all the molecules are surrounded by other molecules such that the forces of attraction are the same within it. However, at the surface of the liquid there are unsatisfied or unbalanced forces resulting in an inward attraction. These forces give a spherical shape to small drops of liquids (Carole Moules, Camtel Ltd.). The contraction

that occurs at interfaces in order to reduce the surface area leads to a state of tension called surface tension. The tension at the surface of one liquid with another liquid is called interfacial tension.

Table: 1. The Surface Tension Values for Different Liquids. *(CRC Handbook of Lubrication: Theory and Practice of Tribiology, Volume II by Robert W. Bruce)*

Liquid	Surface Tension (dyne/cm)
Water	72
Mineral Oil	30-35

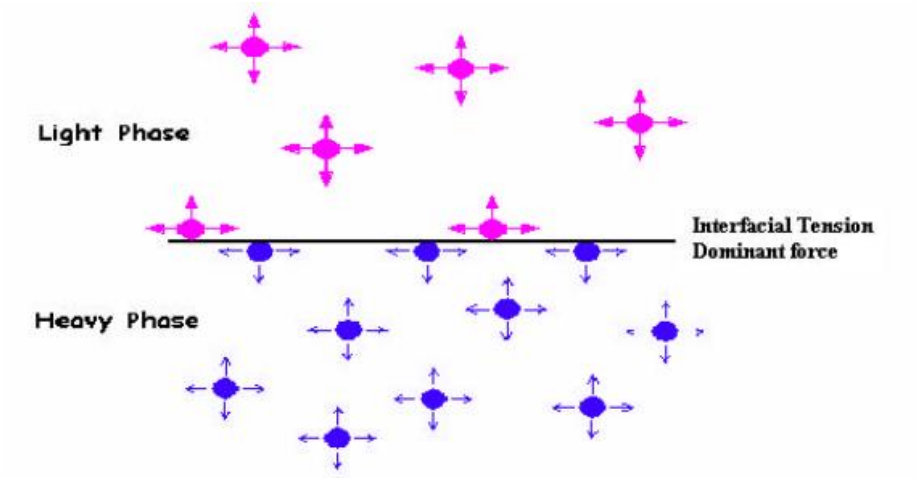

Figure 4: The Interface between Two Pure Liquids along with the Forces of Attraction acting on the Molecules in Both Liquids (Carole Moules, Camtel Ltd.)**.**

2.1.1.3 Spreading Coefficient (S)

The thermodynamic criterion when one liquid (A) can spread and displace a second liquid (B) from a solid surface (S) is given by the spreading coefficient, $S_{A/SB.}$ A positive value of S indicates that spreading will tend to occur.

$S_{A/SB} = \gamma_{S/B} - \gamma_{S/A} - \gamma_{A/B}$ [1]

Equation [1] above calculates the spreading coefficient of 'A' (oil) over 'B' (water), where the γ's are the appropriate interfacial free energies. The spreading that is described in equation [1] is that of the solid (S) / liquid (A) / liquid (B) interface, a three phase system. If the value of S_A/S_B is negative or zero, then liquid (A) which is oil will not displace liquid (B) which is medium (Zettlemoyer, Aronson, and Lavelle 1970).

Table 2. Spreading of Oil on Water Surface *(Source: Bondi, A., Physical Chemistry of Lubricating Oils, Reinhold Publishing Corporation, New York, 1951)*

Oil/Water Interface at 20 ^{o}C	Oil/Air Surface tension (mN/m)	Oil/Water Interfacial tension γ (mN/m)	Oil/Water Spreading Coefficient, S(mN/m)
Mineral Oil	31	53.0	-11.2

In Table 2 above it can be seen that the value of S is negative, which means that oil cannot displace water when it is in contact with a solid surface (glass). The glass surface is the combination of the cell chip and the sensor chip with a gap of 2 µm between them. The principle of interfacial tension along with the spreading coefficient helps in establishing the idea of using mineral oil as a sealing method. Using oil as a medium to seal eliminates the glass on glass approach and the necessity for large weights to produce hermetic seals.

2.2 Creating the Required Design

The design comprises two chips: one chip has wells for the sensors (sensor chip) and the other chip has microfluidic channels and cell traps (cell chip). An existing design for the wells (Kelbauskas et al. 2012) was adopted and used for the sensors. The well dimensions are 20 µm deep, 50 µm inner diameter, 120 µm outer diameter, and 18 µm high. This design was slightly changed later, to incorporate the cell traps of the second chip. The new design had an increased inner diameter of 70 µm so that the cell traps would not be in close contact to the rim of the wells. This prevented the cell traps from breaking off, which was the issue faced earlier due to smaller inner diameter wells.

The design for the channel had a few factors to be considered: one was the size and the shape of the cell trap and the other was the thickness of the channels. The size of the cell traps that is the gap between the two C-shaped structures was close to the size of the single cell, which ranges from 5-18 µm. Different designs for cell traps were considered. **(Figure 5(a))**. It was observed that increasing the number of slots for the trap would make it weak and difficult to fabricate. Also the overall circle diameter had to be 18 µm

to accommodate cells with maximum diameters of 18 µm. The C-shaped design was the final design selected. The channel width was designed to be 100 µm. This width was selected for preliminary experimental studies and simulations can be performed using other values. The chip was designed to have one port as an input and one port as on output. The channels originate from the inlet port and are separated from each other ensuring that any blockage in one channel will not block the flow through the entire chip **(Figure 5(b)).**

Another important factor that had to be considered is a 2 µm gap between both chips which is formed when the channels and the wells are brought together **(Figure 5(c))**.There are two main reasons for having the 2 µm gap:

- One, to ensure diffusion of oxygen into the wells. The use of the two existing technologies (Kelbauskas et al. 2012) in CBDA has shown that a gap of more than 0.5 µm would be sufficient to offset a consumption rate per cell of 1 fmol/min, considering the surface area of the well and the flux of oxygen into the system.

- Two, to allow the flow of medium into the wells when the two parts of the chip are in contact. Without the gap, the medium will not enter the wells and it will not serve the purpose of flowing liquids through the system without separating the two chips. The gap enables easy and rapid entry and exchange of the medium into the wells.

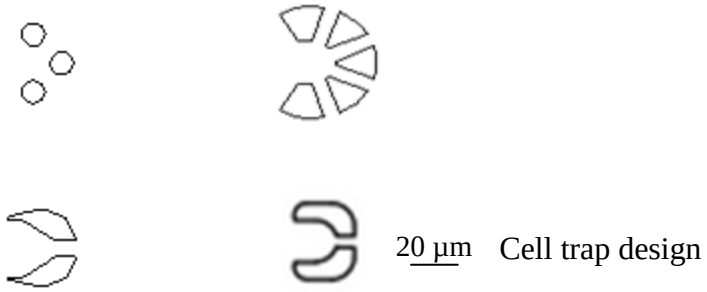

(a)

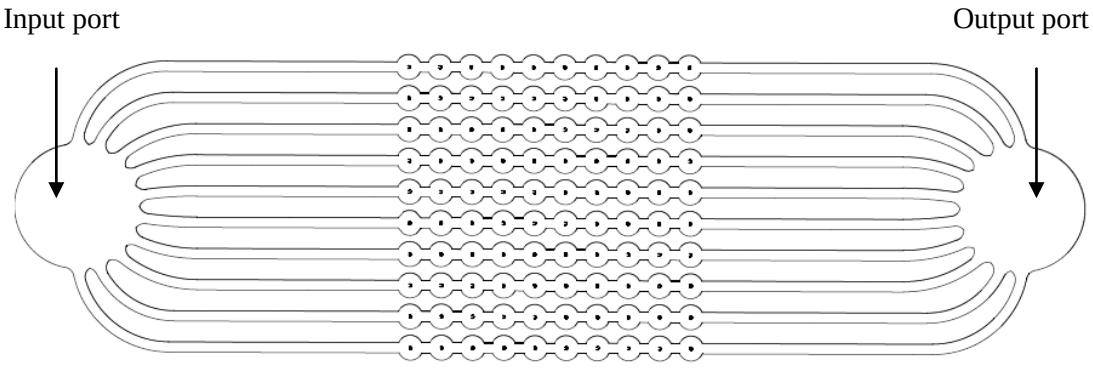

(b)

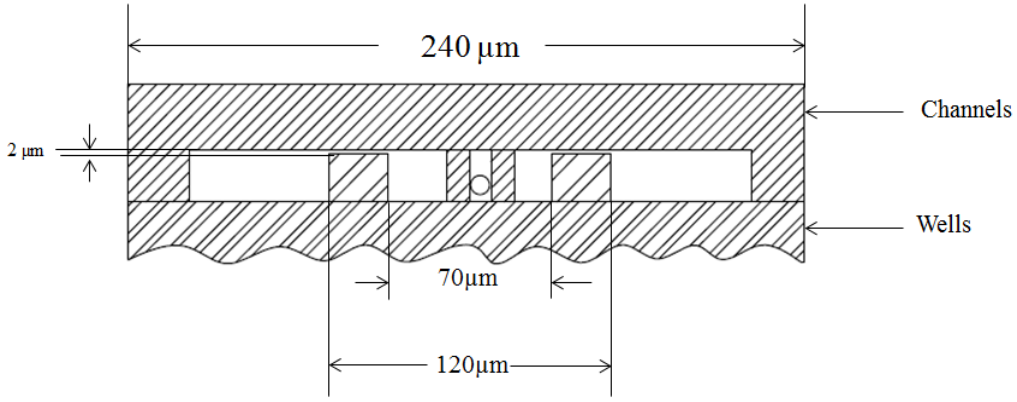

(c)

Figure 5: The Proposed Design for the Channel with the Cell Trap. (A) The Different Designs for the Cell Traps. (B) The Channel with the Input and Output Ports. (C) A Cross Section of the Cell Chip and the Sensor Chip Sealed Together.

2.3 Implementation

The properties of mineral oil stated in Section 2.1.1., are used in designing a method to attain a proper seal for single cell analysis. A seal is needed to measure oxygen consumption rates of single cells in wells. If it is possible to replace the oil with fresh medium as well as buffered media and drugs, single cell environmental and drug response assays can be performed. It may also be possible to perform end-point analyses such as gene expression. The chip is designed to allow easy and efficient replacement of fluids within the microfluidic channels as follows:

Figure 6 is an illustration of a sequential flow of two liquids (medium and oil) into the channel. The test begins by flowing the medium (green color) into the system. The medium enters into the wells and around the channel. This ensures that the cells have the required amount of oxygen through the medium within the wells. The oil (red color) then enters the system and flows through the channel, but does not enter into the wells due to the surface tension at the medium/glass/oil interface. This helps in maintaining a seal around each well. After the oxygen consumption rates of these cells have been determined by performing a drawdown test (test to find oxygen consumption rates), the cells can be used for further analysis. This requires the system to be flushed with fresh medium. So in the next step, fresh medium (blue color) is introduced into the system which flushes out the oil and replaces the medium within the wells.

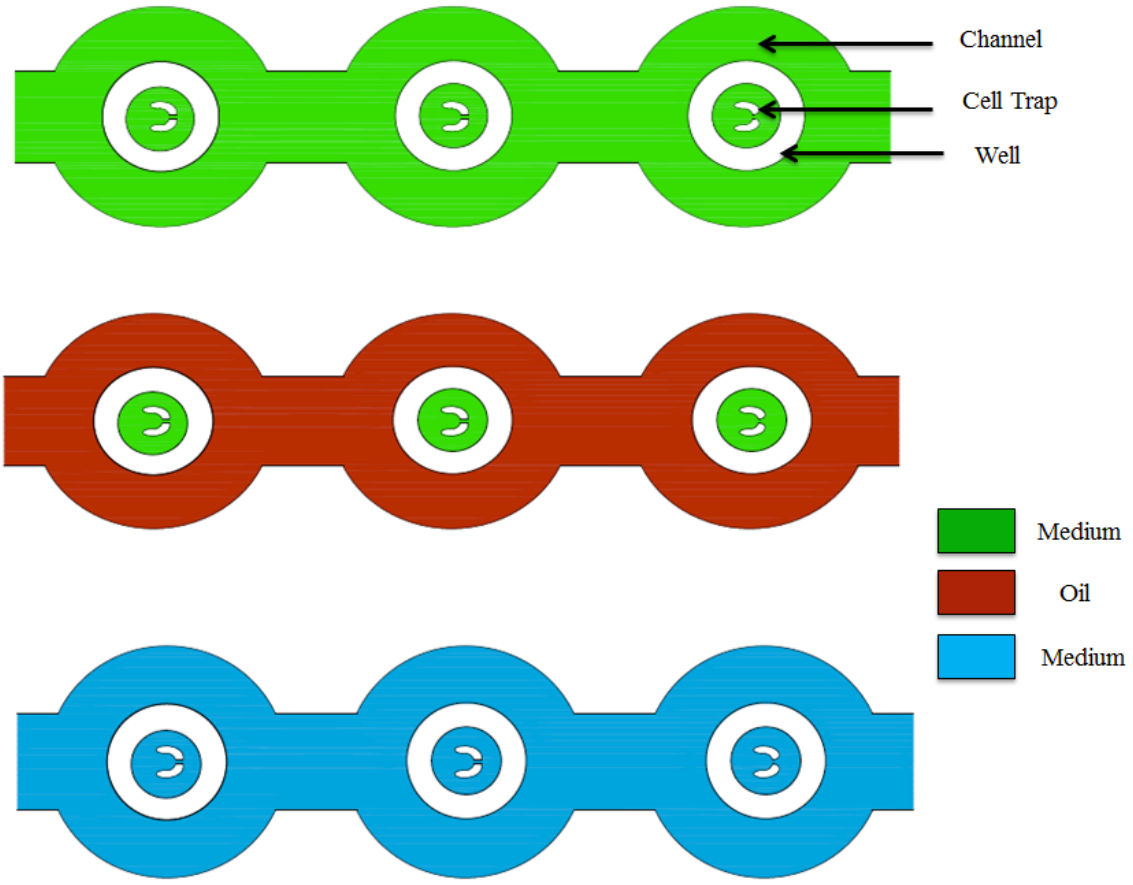

Figure 6 : A Diagrammatic Illustration (Top View) of the use of Medium and Oil in a Section of the Fluidic Channel.

Figure 7 shows a cross section of the channel along with the 2 µm gap between the two chips. This gap allows the easy exchange of the fluids. This is a diagrammatic explanation of the flow, along with the medium and oil in the channel.

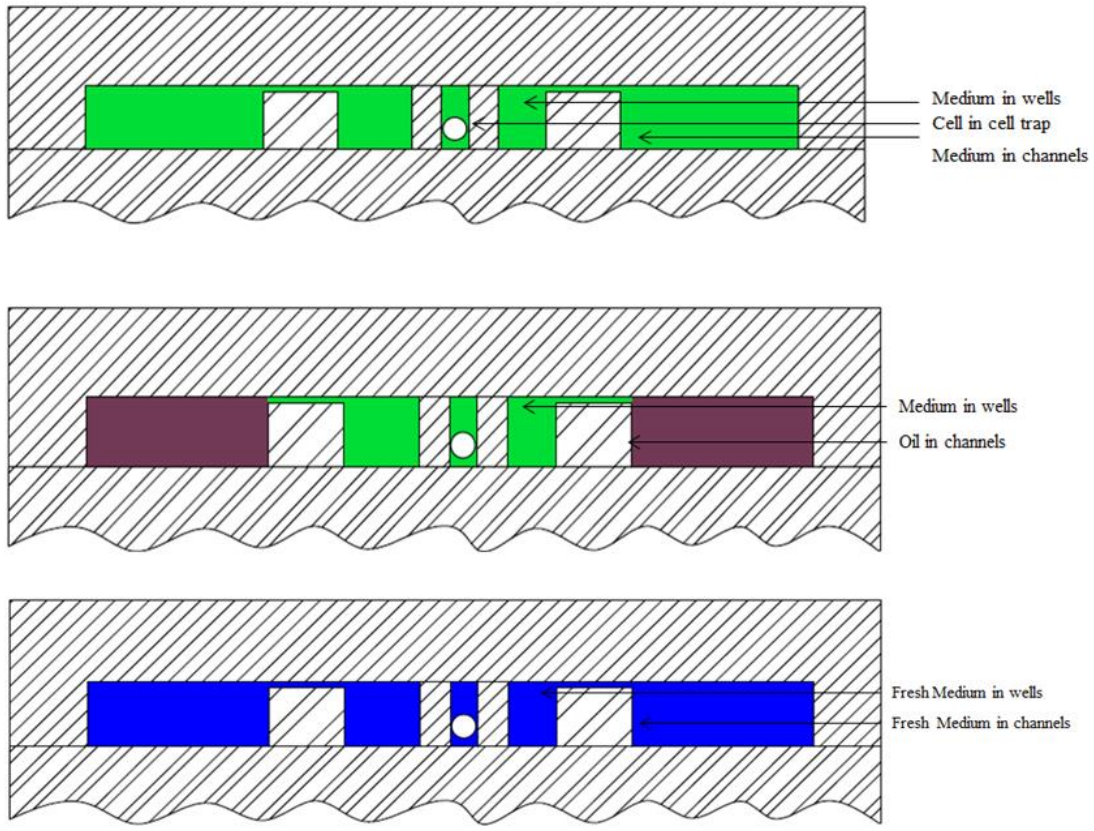

Figure 7: A Vertical Cross Section (Side View) of the Fluidic Device with the Sensor Chip on the Bottom and the Cell Chip on Top of it.

2.4 Practical Implementation of Exchange Between Two Fluids

The chip (cell chip and sensor chip assembly) was tested to evaluate the ease with which fluid exchange takes place within the channel and the wells. The test was performed by using an inverted microscope (Nikon Eclipse TS100, Melville, NY) which has a camera for imaging of the fluidic channel. The experiment uses water as an aqueous medium. Water and oil were stained with two different colors to distinguish their flow within the channel. The water used had two colors: green and red. The oil was red. Green water flows through the channel and enters into the wells because of the 2 μm space that is

present between the two chips once they are aligned and sealed together **(Figure 8(a))**. The red oil is then made to flow through the device, where the oil flows only through the channels and does not enter into the wells, even though there is a 2 µm gap between the two chips. This shows that oil flows through the system but does not displace the water inside the well because of the negative value of the separation coefficient, (Interfacial Properties of petroleum products by Lilianna Z. Pillon, CRC Press) **(Figure 8(b))**, which helps in providing a seal around the wells. Red water is then flown into the device to see if it can displace the water inside the wells. It is observed in **Figure 8(c)** that the water flushes out the red oil and replaces the green water inside the wells. This proves that the two fluids can replace each other easily and without causing the oil to enter the inside of the wells. The whole exchange between these fluids takes only 30-60 seconds.

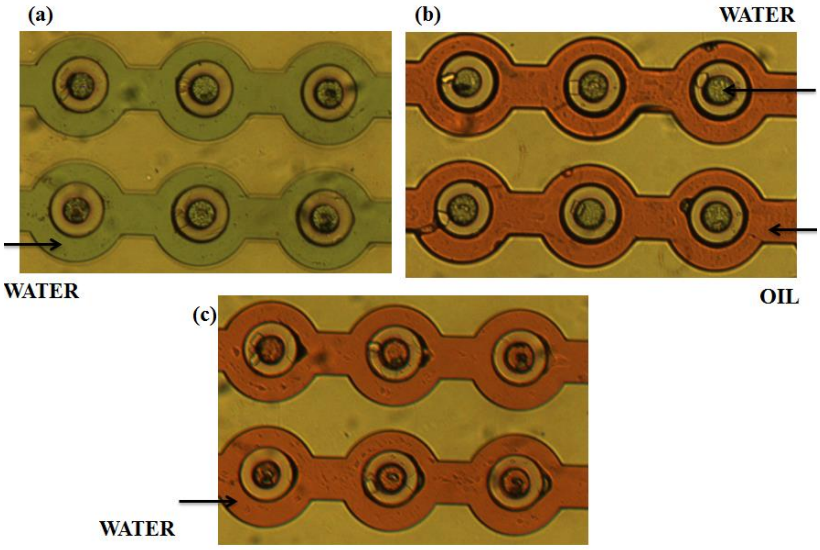

Figure 8: View of a Section of the Channel under an Inverted Microscope.

CHAPTER 3: DEVICE TESTING

3.1 Experimental Setup

A few steps need to be followed before the drawdown test is performed. The drawdown test is where the OCR measurements for the single cells are performed. The chip which has the cell traps and the channels (cell chip) needs to be loaded with cells. The oxygen detecting sensor is deposited into the second chip with wells (sensor chip). The two chips are then aligned with each other using an x-y-z controlled stage in such a way that each well encloses a single cell in the trap.

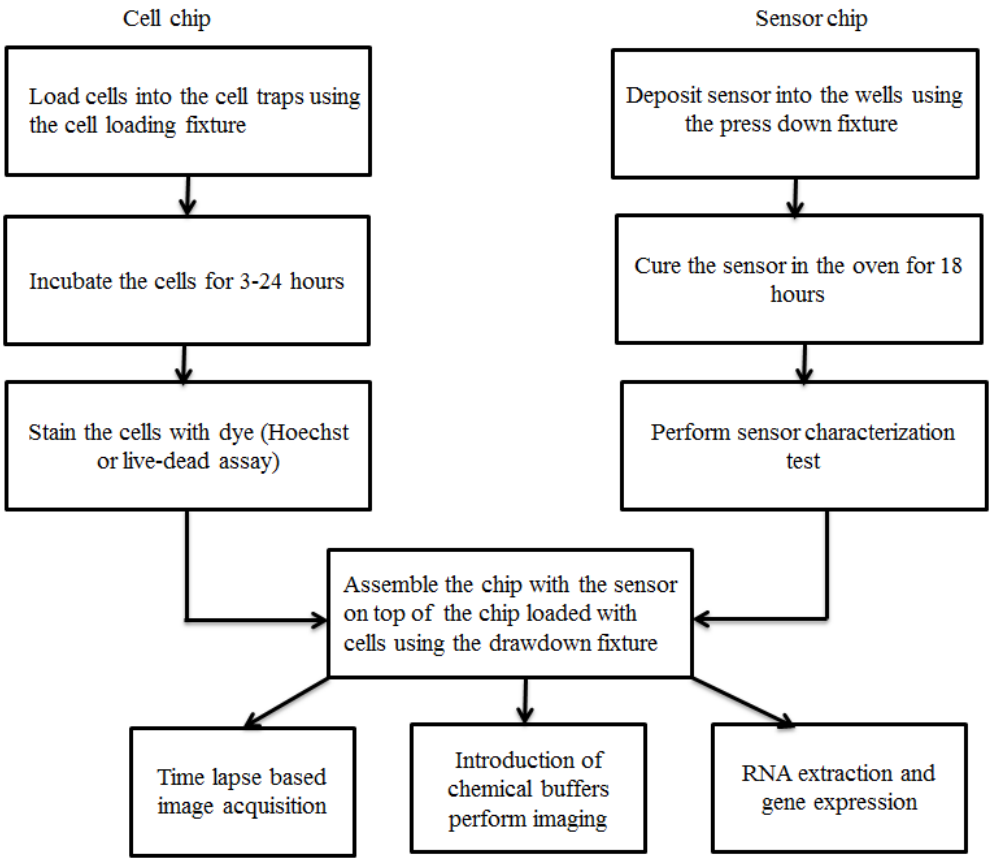

Figure 9: Flow Diagram of the Experimental Setup.

The flow diagram in **Figure 9** shows the steps starting from cell loading and sensor deposition to the final drawdown measurements with the intermediate steps.

3.2 Cell Loading into Cell Traps using Cell Loader

3.2.1 Cell Culture

For this study we used the immortalized human esophageal epithelial cell line, CP-A, which was derived from patients with Barrett's esophagus without dysplasia (Kelbauskas et al. 2012). CP-A cells are maintained in a 37ºC incubator with humidified atmosphere of 5% CO2. The complete growth medium in which the CP-A cells are cultured is Keratinocyte SFM cell growth medium supplemented with human recombinant epidermal growth factor hEGF (Peprotech, Rocky Hill, NJ) at 2.5 µg/500 mL, bovine pituitary extract at 25 mg/500 mL, and penicillin/streptomycin solution(Invitrogen) at 100units/100µg/mL. The cell culture process which is followed by a cell culture specialist is as follows:

1. CP-A cells are cultured in T-25 flasks (Corning, NY) until they are approximately 80% confluent.
2. They are washed using Dulbecco's Phosphate Buffered Saline (DPBS). The wash solution is removed from the culture vessel.
3. The cells are trypsinized using trypsin-ethylenediamine- tetraacetic acid (EDTA) solution 1 mL pre-warmed 0.05% trypsin at 37^{o}C for 5-8 minutes.
4. An equivalent of 2 volumes (twice the volume used for the dissociation reagent) of pre-warmed complete growth medium is added to the flask.

5. Cells are transferred to a 15 mL conical tube and centrifuged at 900 rpm for 3 minutes. The cells are resuspended in 1 mL of pre-warmed complete growth medium and a sample is removed for counting. The total number of cells and percent viability are determined by trypan blue exclusion using a Countess® Automated Cell Counter.

6. The cell culture specialist provides 100,000 cells in 3 mL of medium for the cell loading procedure.

3.2.2 The Chip with Cell Traps

The chip with cell traps has microfluidic channels along with cell traps fabricated using negative photoresist (SU-8/KMPR) on 500 µm thick fused silica substrates. Each substrate contains 25 chips. The size of the chip is 16 mm x 11 mm. The chip has ten channels where each channel is 10 mm long. Every channel has 10 cell traps in it and the distance between each cell trap is 18 µm. The maximum size of cells that can be trapped in a trap is 18 µm. At the four corners of the chip there are circular structures which act as a locking system while assembling the chip onto the second chip with wells during drawdowns. **(Figure 10(a)).** The cross section shows the channel and the cell trap with a cell trapped in it. The height of the channels with the cell traps is 20 µm **(Figure 10(b)).**

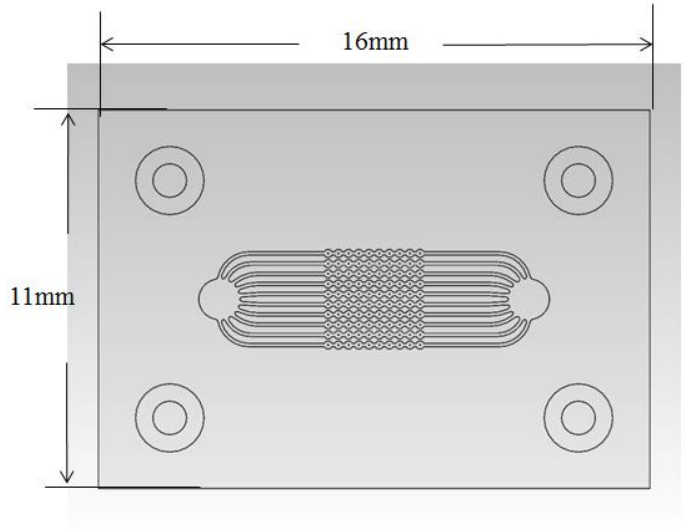

(a)

(b)

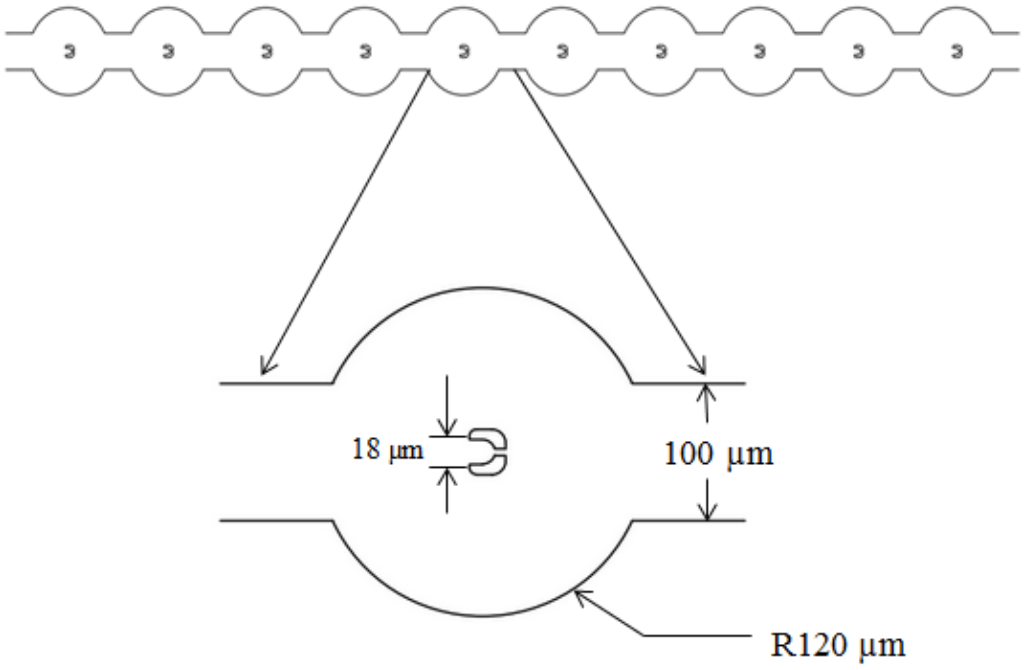

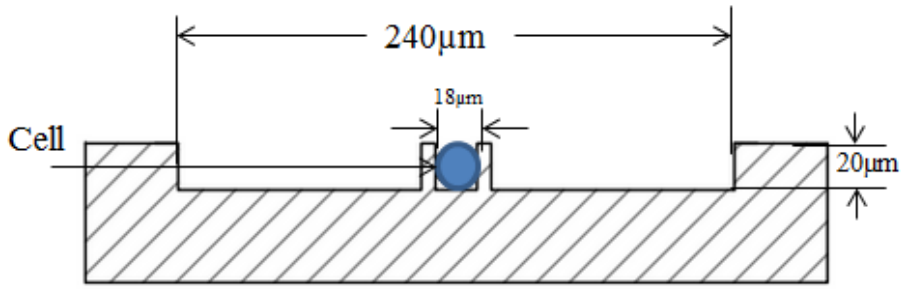

(c)

Figure 10: Chip Design. (A) The Entire Chip with Channels and Cell Traps. (B) A View of a Single Channel with the Cell Traps in it along with an Enlarged Picture of a Cell Trap. (C) Vertical Cross Section through the Channel and the Cell Trap.

3.2.3 Cell Loader and Cell Loading Process

The cell chip is loaded by using a microfluidic platform to flow cells into the chip. This is achieved by using a fixture that will hold the chip in it, which is then placed in the field of view of the microscopic objective. The microfluidic fixture provides two ports to the system: one port is the inlet and the other is an outlet **(Figure 11(a)).** Before cells are loaded into the syringe, they are first filtered using BD Falcon™ tubes. These tubes are 5 mL polystryene round bottom tubes with a cell strainer cap. The cell loading process begins with loading two syringes of 3 mL volume each, one with cell medium and the other with the CP-A cells (100,000 cells in 3 mL medium). The syringe with the medium has a filter with a 0.8 µm Supor® Membrane (Life Sciences Acrodisc® 25 mm Syringe Filter) attached to it. The filter removes the debris in the medium which will prevent any unwanted particle from blocking the channels or getting trapped into the cell traps.

The two syringes are now attached to a three-way valve which is then connected to the inlet of the system **(Figure. 11(b)).** The chip is first primed and then made to sit on the acrylic fixture. A PDMS layer and acrylic piece are placed on top. The whole system is then assembled using screws . The whole fixture is then placed on an inverted microscope for routine microscopy (Nikon Eclipse TS100, Melville, NY) to view the flow of cells in the channel. Using the three-way valve, the medium is first made to flow through the system. The flow rate is manually controlled, but a flow pump could be integrated into the system to automate flow control. After medium fills all the channels, the valve is closed so that cells can flow through the system. The cells are made to flow through the channels at a particular rate such that they get trapped. Presently, 100% occupancy is achieved by flowing 3 mL of cells in a period of 1 minute through the system. After the cells are loaded into the traps, the chip is then flushed with medium to remove the excess cells present in the channel. Once the chip is loaded, it is then placed in the incubator under normal physiological conditions for 3-24 hours to allow cell adhesion to the surface. During incubation, medium is continuously flowed inside the incubator to ensure that the cells have access to nutrients and oxygen.

The chip is removed from the fixture before it is assembled for running the drawdown test. The cells undergo a cell viabilty test to quantify the number of cells that are alive and dead. This is performed by using a Live-Dead Cell Imaging Assay (Molecular Probes by Life Technologies, Grand Island, NY). Then the incubated cells are stained with Hoechst 33342 dye (Life Technologies, Molecular Probes®, Grand Island, NY) and viewed using transmission bright field imaging. The cells that are dead after incubation are excluded from data analysis.

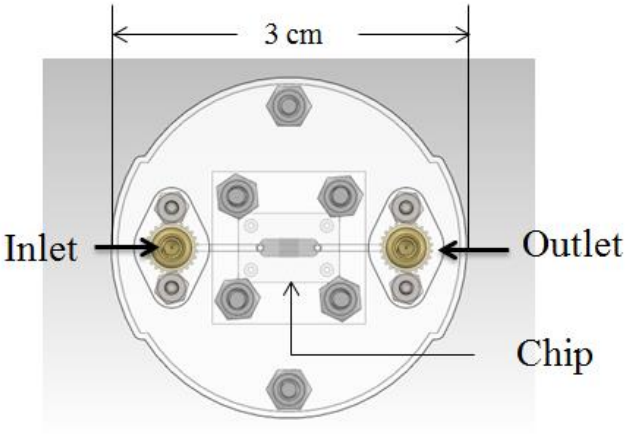

(a)

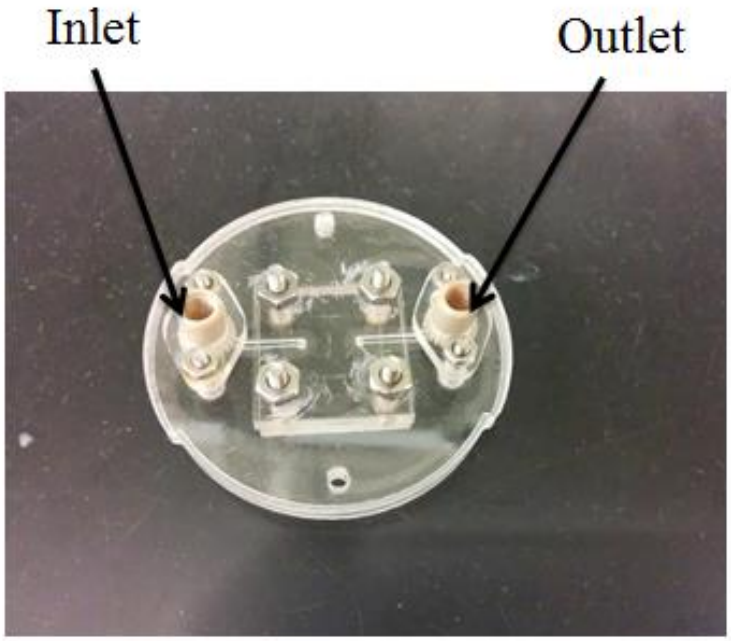

(b)

(c)

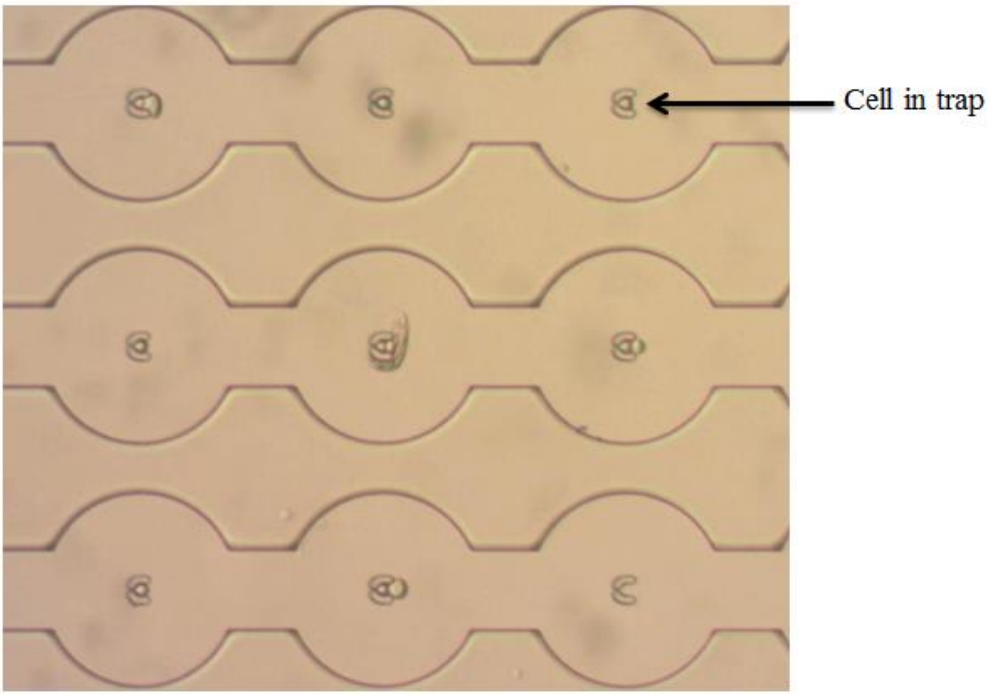

Figure 11: The Chip within the Microfluidic Fixture. (A) The Diagrammatic Representation of the Fixture. (B) Experimental Setup of the Cell Loader. (C) Image of Individual Cells Captured in the Traps using an Inverted Microscope.

3.3 Deposition of Sensor into the Wells

3.3.1 Well Design

The second chip which forms the top half of the device, the sensor chip, has wells fabricated in fused silica substrates which are 500 µm thick and coated with chrome which acts as a masking layer using negative photoresist lithography and chrome-etch technique. A total of 25 chips can be fabricated in each substrate. The size of the chip is 16 mm x 11 mm. The chip has a 10x10 array of wells. The size of the array is 3 mm

having a distance of 300 µm between two adjacent wells. Each well is made of an outer circle with a diameter of 120 µm and an inner circle with a diameter of 70 µm. Each well is 18 µm deep with a height of 18 µm **(Figure 12(a))**.

Two holes of 1 mm diameter are drilled into the chip at a distance of 11.5 mm from each other by using the MB-1000 XCALIBER, a precision multilaser micromachining platform by Potomac. These holes are the input and the output ports for the microfluidic system while performing drawdown tests. At the four corners of the chip there are circular structures which are used to lock the system while assembling the chip onto the cell traps during drawdowns. The cross section shows the depth of the wells along with the lips that surround the wells **(Figure 12(b)).**

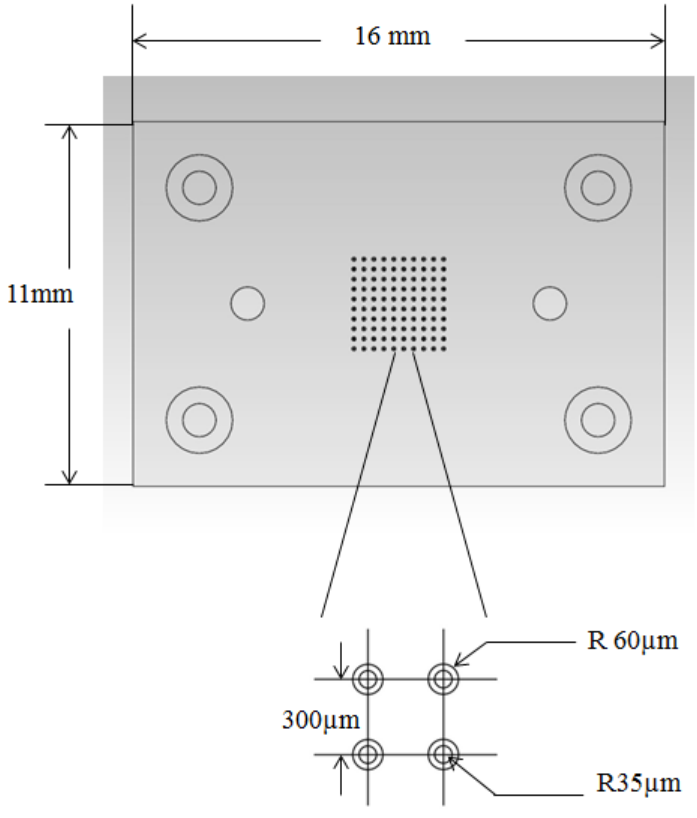

(a)

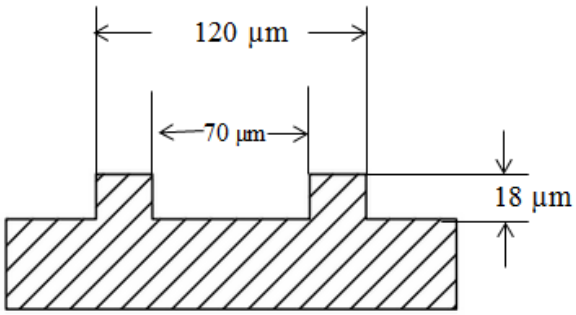

(b)

Figure 12: Sensor Chip Design. (A) The Entire Chip with Wells and a View of Wells with the Lips with the Cell Traps in it along with an Enlarged Picture of a Cell Trap. (B) Horizontal Cross Section through the Wells.

3.3.2 Sensor Deposition into Microwell

A sensor is deposited into the microwells to measure the oxygen concentration within the wells. The oxygen consumption rates for single cells in each well are calculated using a self-referencing, dual pH and oxygen ratiometric sensor, which measures the sensor emission intensity. An advantage of this sensor is that the signal is independent of the sensor volume. This study deals with extracellular sensing, in which case the sensors are in the format of crosslinked polymeric hydrogels. The sensor used is composed of three probes: an oxygen probe, a pH probe and an internal built-in probe (reference probe) which is inert to pH and oxygen [17]. Oxygen concentrations are measured by monitoring the fluorescence intensities at 650 nm. The pH concentrations can be measured by observing changes in fluorescence intensities at 521 nm [17]. The drawdown experiments performed in this thesis produced single-cell oxygen

consumption rates, but they could also be used to monitor the change in pH values for single cells.

3.3.2.1 Preparation of Lids

There are a few steps that need to be followed prior to depositing the sensor into the wells. These steps are followed so that the sensor reliably adheres to the surface of the wells.

- The lids are placed into a petri dish and acetone is added to it. The dish is then agitated for 2 minutes. This removes impurities and particles from the lid.
- The lids are then rinsed off using reverse osmosis (RO) water to remove acetone.
- The lids are then placed in a beaker with Micro 90 solution for further cleaning. This beaker is then placed in a sonicator to sonicate for 30 minutes.
- The lids are then dried using a nitrogen gun and then plasma-cured for 30 minutes. The plasma curing makes the lid surface hydrophobic.
- The lids are then placed in a desiccator with silane (3-Acryloxypropyl Trimethoxy-Silane) for at least 3 hours. Silane vapor gets deposited on the glass surface of the wells. This assists in binding of the sensor onto the glass surface.

3.3.2.2 Sandwich Method used for Sensor Deposition

The microwells are 18 µm deep and 70 µm wide. An acrylic fixture is used to deposit the sensor into the microwells using the sandwich method, where a drop of sensor is deposited onto the lid and pressed with a glass lid. The lids are placed on a layer of

PDMS, which is on an acrylic fixture. Then 1 µL of sensor is deposited on top of the lid and a glass slide is placed on top of the lid, followed by the above acrylic piece of the fixture. The two pieces are then brought together using screws. The PDMS layer in between the two acrylic pieces prevents the lid from cracking due to the force caused while tightening down the fixture. This process causes the sensor to also enter, undesirably, into the interstitial area between wells **(Figure 13(a))**. The fixture is placed in a beaker with water and left to sonicate for 15 minutes. This process removes the excess sensor deposited in the interstitial area. The whole fixture is then placed in an oven at 80^{o} C for 18 hours to cure under a 100% nitrogen atmosphere. During this period, the sensor polymerizes.

(a)

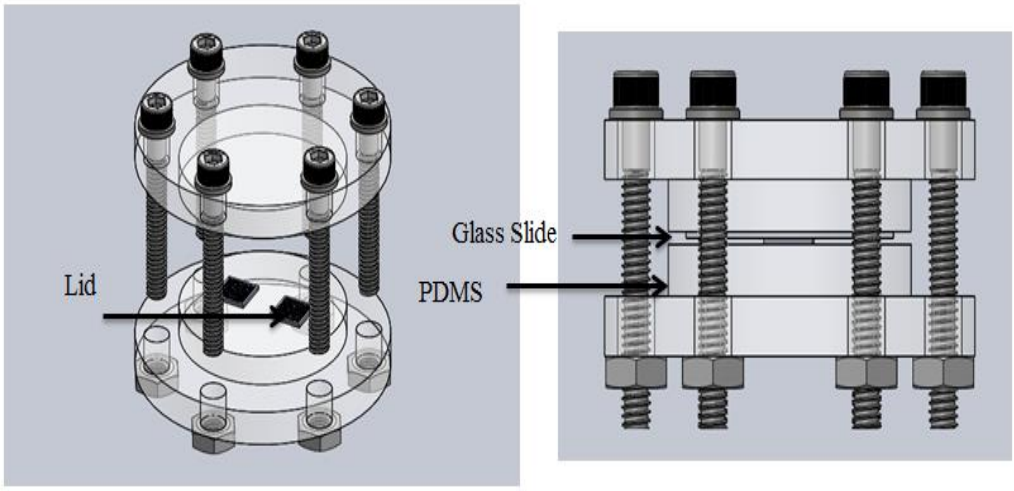

(b) 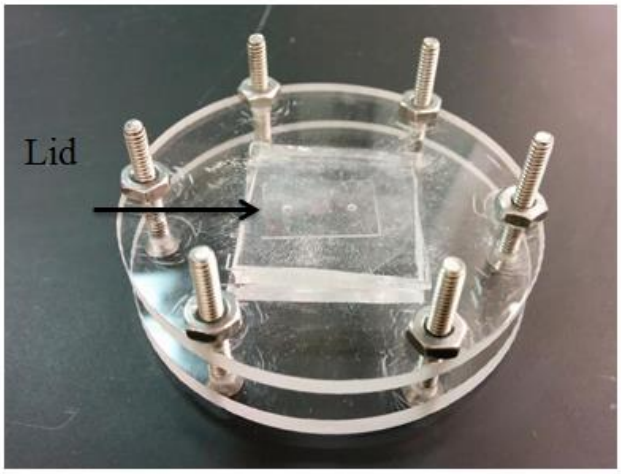

Figure 13: The Sensor Deposition Fixture. (A) A Diagrammatic View of the Different Layers Present in the Fixture. (B) The Actual Fixture with the Lid Sandwiched in between.

3.4 Assembling Both Chips for Drawdown Experiments

To perform drawdown experiments on single cells, the two chips must be assembled on top of each other, the cell environments sealed, and the chips imaged to obtain the sensor information. The chips must be tested individually before they are assembled for the drawdown experiments. The sensor chip needs to undergo a sensor characterization test and the cell chip undergoes a cell viability test. The sensor characterization test determines the sensor response to changes in oxygen levels. The cell viability test as explained earlier, quantifies the number of live and dead cells in the chip.

The drawdown fixture is the device that holds both the chips, wells and cells **(Figure 14(a))**. It also provides the input and output ports to the chip. These ports are used to introduce medium and oil into the chip. The fixture is made of acrylic and is 7.5 cm x 5

cm. There are two acrylic structures, one that is rectangular which holds the wells and one that is circular and holds the chip with cells. The base structure also has channels which flow from the input and output ports of the fixture to the input and output ports of the sensor chip. PDMS layers are used in between the two acrylic structures to distribute the force evenly across the chip assembly and prevent any breaking or leakage in the device.

(a)

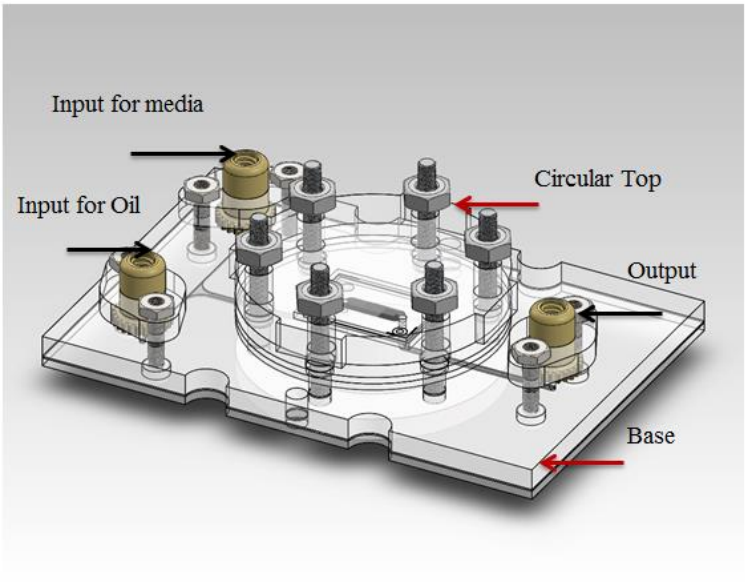

(b)

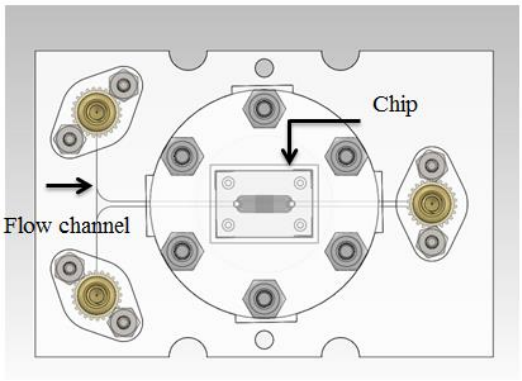

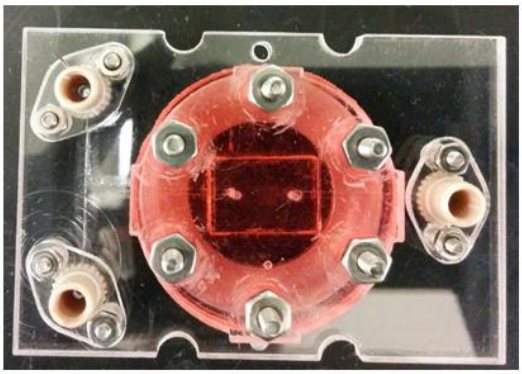

Figure 14: (A) The Drawdown Fixture with the Input and Output Ports. (B) The Diagrammatic and the Actual Fixture with the Chips Mounted in it.

3.4.1 Chip Assembling Unit

The chip assembly requires alignment of the wells with the traps so that the wells enclose the cell traps. Manual chip assembly using the microscope is very difficult and time consuming. This may affect the cells since they had to be out in the open for a

longer duration of time. To overcome these difficulties, a semi-automated assembling unit was made. The unit sits on the stage of the microscope and the two chips are mounted on the assembling unit. The microscope used is an inverted microscope (Nikon Eclipse TS100, Melville, NY). The entire assembly (the two chips) is mounted upside down using the unit, i.e. the movable sensor chip (top) and the stationery cell chip (bottom). Using the knobs on the unit, the sensor chip can be moved along all three axes, x, y, and z, to accurately align it to the cell chip on top of each other. **(Figure 15(a))**. Once the two chips are locked into each other by using the structures at the four corners, then two acrylic parts are screwed together by using a metal ring and screws.

After assembling the two chips on top of each other, the drawdown fixture is then removed from the assembling unit and mounted on a plate **(Figure 15(b))**. This plate holds the two chips for the drawdown. The plate is then placed on the stage of an inverted microscope (Nikon TE 2000-E) that is used for the drawdown test. This microscope is used for measuring the fluorescence response from the sensor.

(a)

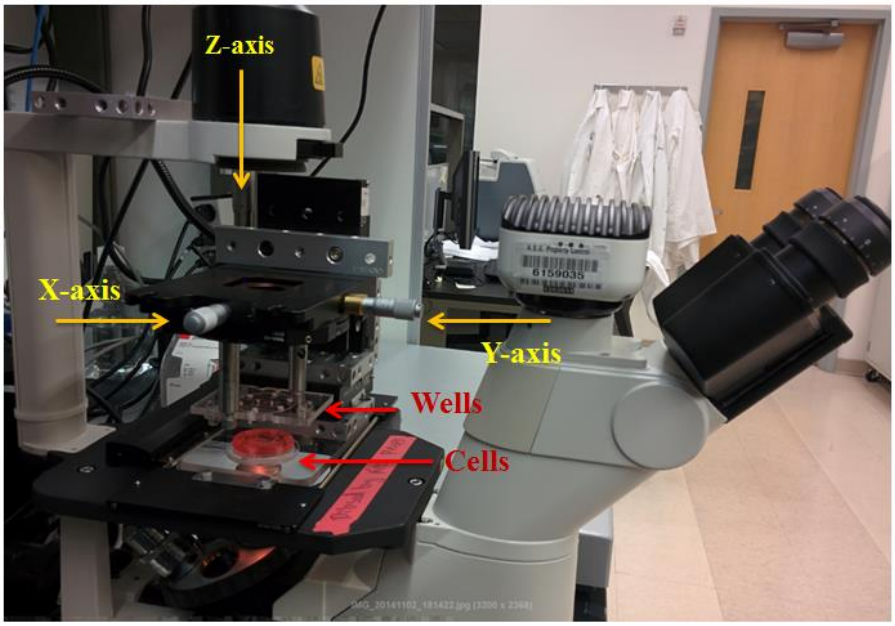

(b)

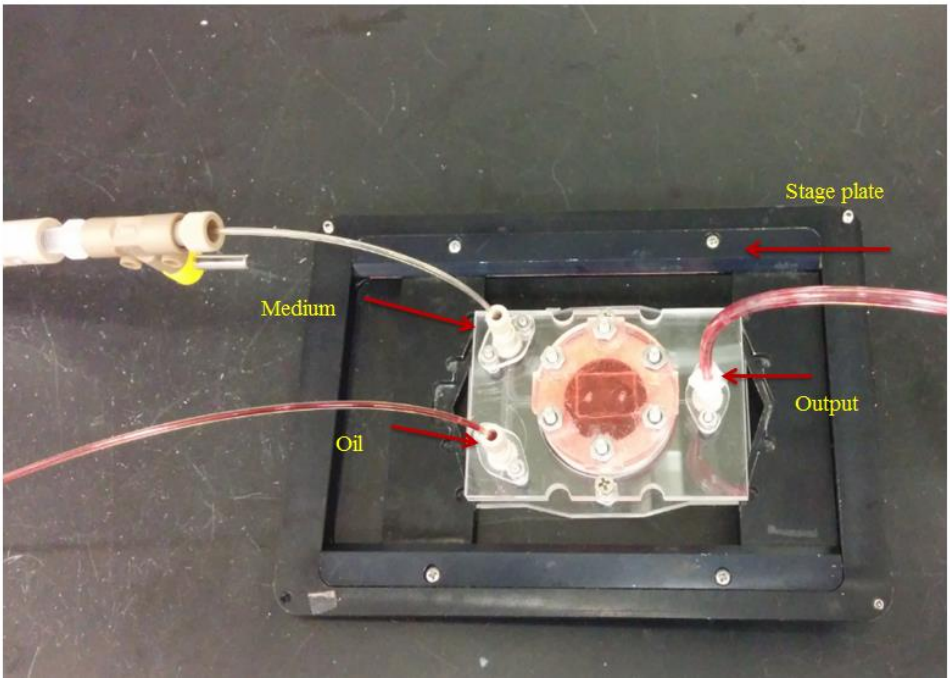

Figure 15: The Setup of the Chips Mounted on the Assembling Unit. (A) The Assembling Unit is placed on the Stage of the Inverted Microscope. (B) The Device Mounted on the Plate for the Microscope.

3.4.2 Drawdown Setup

The OCR measurements are performed on an inverted fluorescence microscope **(Figure 16(a))** (Nikon Eclipse TS2000-E, Melville, NY). This microscope has a custom environmental chamber built around it with a controlled temperature of 37^{o}C to maintain a proper environment for the cells. The two chips are assembled completely and medium and oil is made to flow through the device (drawdown fixture). The drawdown device **(Figure 15(b))** is placed on the stage of this microscope. The microscope stage is controlled with an XYZ automated stage controller which helps in positioning of the drawdown device. The sensor is excited using a narrow band LED operated in a pulse mode in synchronization with the camera. The sensor emission photons at 650 nm are collected using a 10X, NA 0.45 dry objective lens and a dichroic mirror. Sensor emission images are then collected using a high resolution CCD camera for fluorescence imaging (Cool SNAP HQ, Photometrics, Tucson, AZ). Images are captured every minute for 120 minutes **(Figure 16(b))**. The sensor data is then extracted from the images and further analyses are performed on the data.

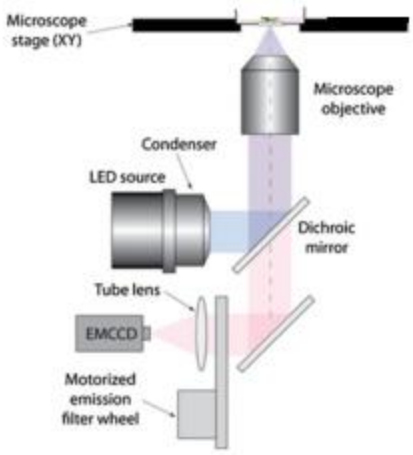

(a)

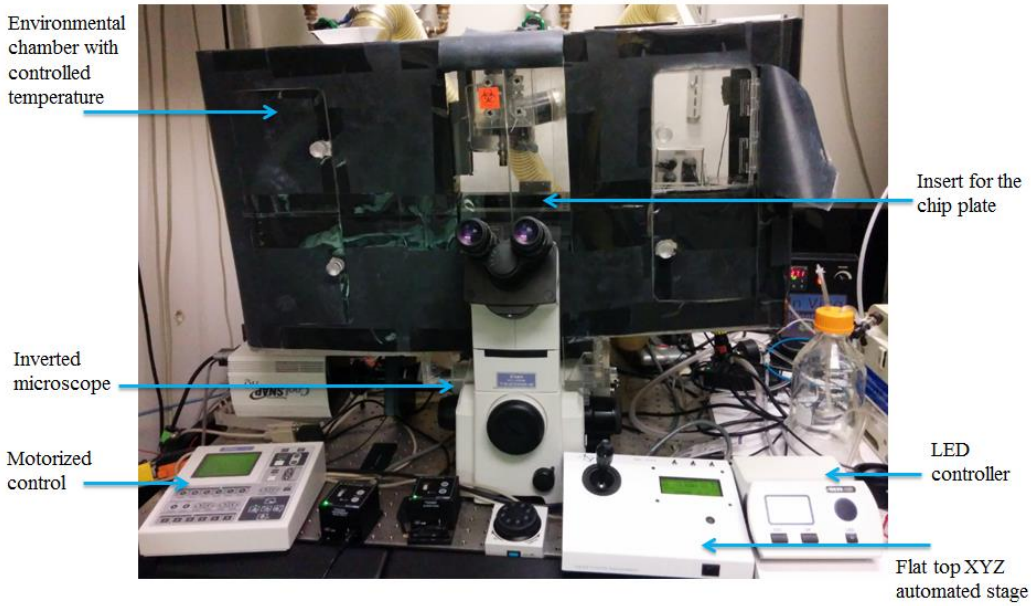

(b)

Figure 16: The Experimental Setup for Measurements of Oxygen Consumption Rates. (A) The Working of the Inverted Microscope used for Drawdown Experiments *(Kelbauskas et al. 2012)***. (B) The Setup of the Entire Experimental Stage.**

CHAPTER 4: RESULTS

4.1 Sensor Deposition Data

After the sensor chips are prepared, a few preliminary tests need to be performed on the chip before it is used for drawdown experiments. The first test is to determine the amount of sensor that is deposited in the wells during the sandwich method. A surface profiler (Veeco Dektak 150) is used to measure the sensor profile on the surface of the chip. This test is performed to determine the amount of sensor in the wells and in the interstitial areas. First the profiler is used over the empty chip and then over the chip with the sensor to determine the final amount of sensor in the wells **(Figure 17(a))**. The second test is the sensor characterization. This test measures the sensor response to changes in oxygen concentration by providing low O_2 levels which are below the limit of detection (168 ppb). Oxyrase (Oxyrase®-Nature's AntiOxidant®, Mansfield, OH) is added to a system which is isolated to provide low O_2 levels (Ho KC et al. 2003). Images are acquired at 30 second intervals. It is seen in the graph, after the introduction of Oxyrase at time point 10 (5 minutes) that there is a gradual increase in the signal. This change in signal indicates that the sensor responds to the introduction of Oxyrase as expected **(Figure 17(b))**.

(a)

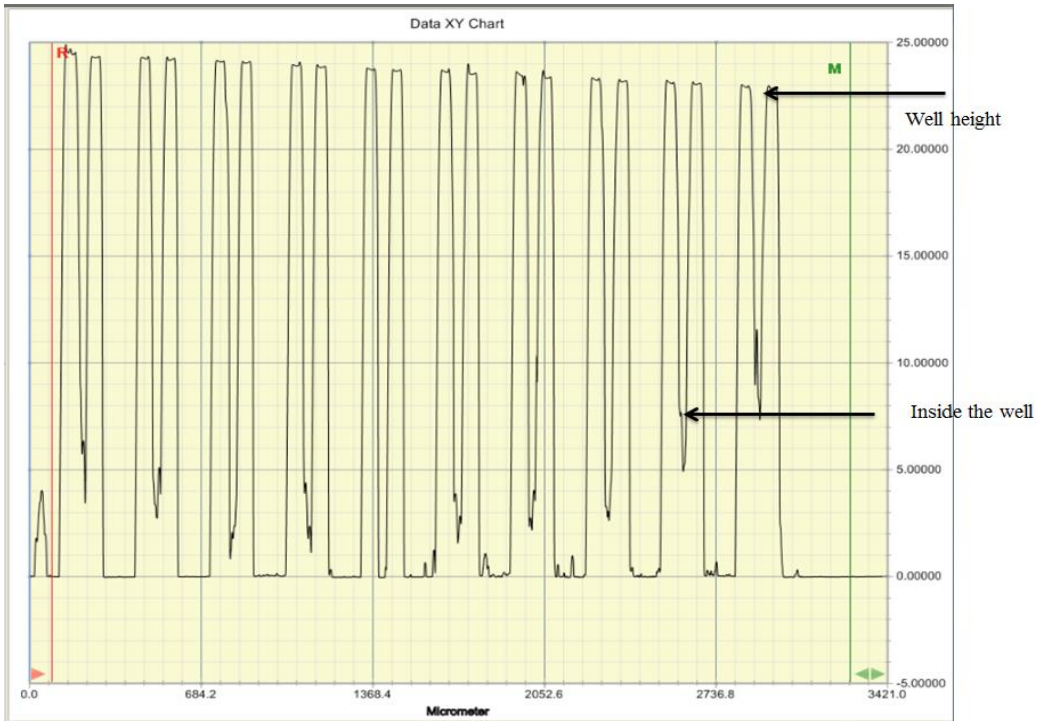

(b)

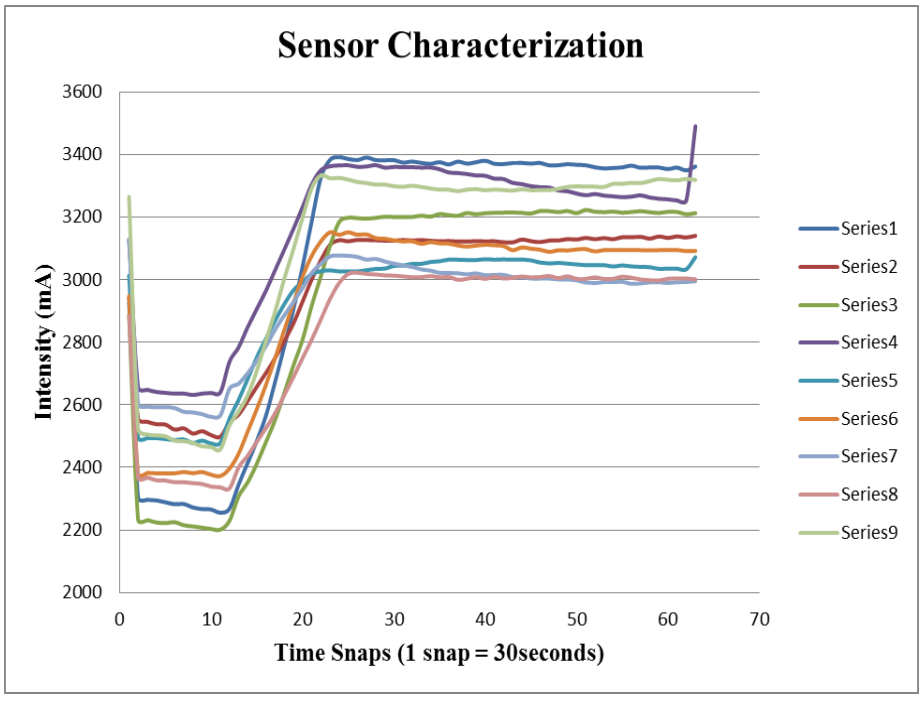

Figure 17: Result of Test Performed on Sensor Chip. (A) The Surface Profile of the Chip. (B) Sensor Characterization Response.

4.2 Cell Viability and Occupancy Rate

The cell loader assembly is used to load cells into the cell chip. After cell loading, the cell loading fixture is placed in an incubator for 3-24 hours. Before the cells are used for drawdown experiments, they are first tested for viability and cell occupancy. The cell viability test is important since only cells that are alive are considered for data analysis. The cells are stained using a fluorescent live/dead cell assay (LIVE/DEAD® Cell Imaging Kit (488/570), Life Technologies, Grand Island, NY) It is a sensitive two color fluorescence cell viability assay in which green indicates live cells and red indicates dead cells **(Figure 18)**. The images are viewed with a fluorescence microscope (Floid® Cell Imaging Station, Life Technologies, Grand Island, NY).

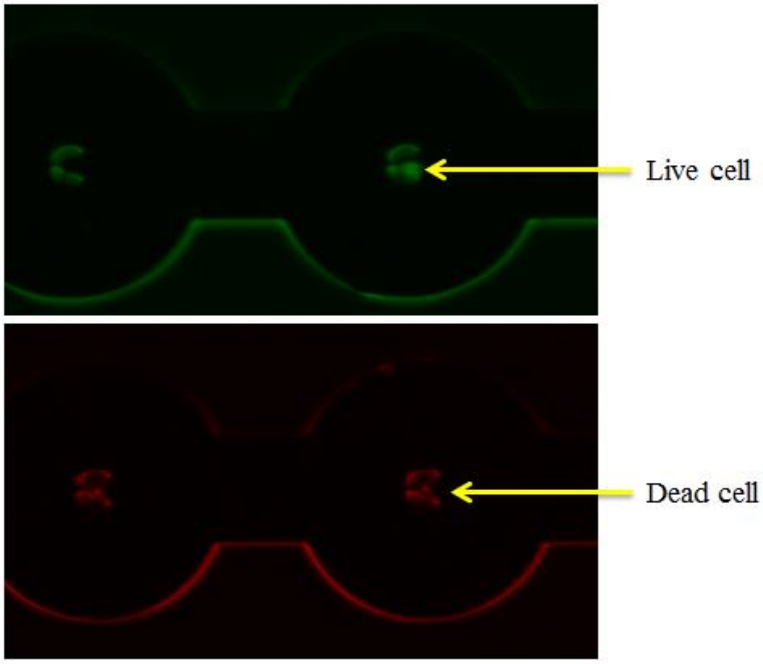

Figure 18: Pseudo Colored Images of Live/Dead Stain in Cell.

The cell occupancy is the number of cells trapped in the cell chip. Cell occupancy rate depends on the number of traps available on the chip and the concentration of the cells during the loading process. This is measured by staining the cells with Hoechst 33342 (Life Technologies, Molecular Probes®, Grand Island, NY), a nucleic acid stain. The stained cells are observed under a fluorescence microscope **(Figure 19)** where the bright spots are cells. The images acquired from these stains are used to determine the cell occupancy rate. This test can only determine the presence of cells, not if the cells are alive or dead. The staining of the cell helps in data analysis by correlating a sensor response to the presence of a cell (live or dead) in a well.

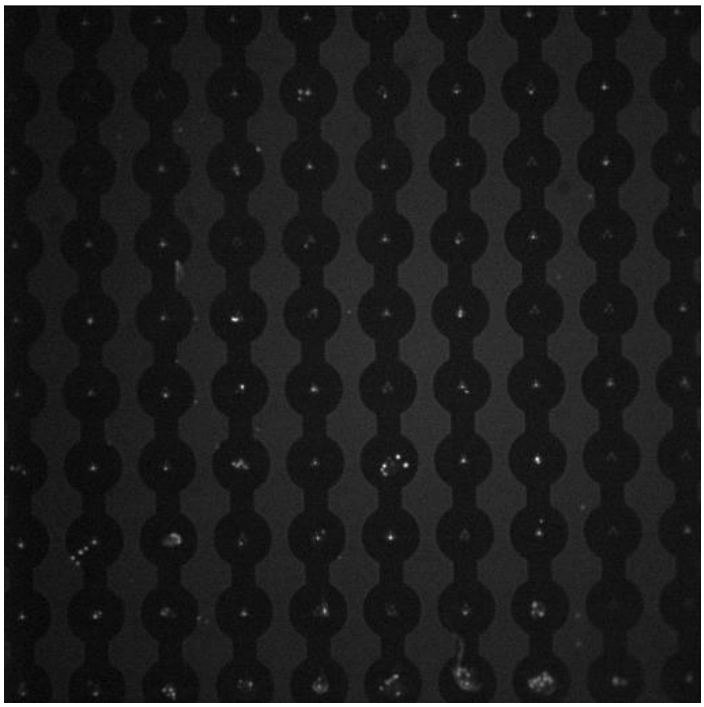

Figure 19: A Fluorescent Image of Cells Stained with Hoechst 33342 Dye.

Table 3: Cell Occupancy Data for CP-A Cells.

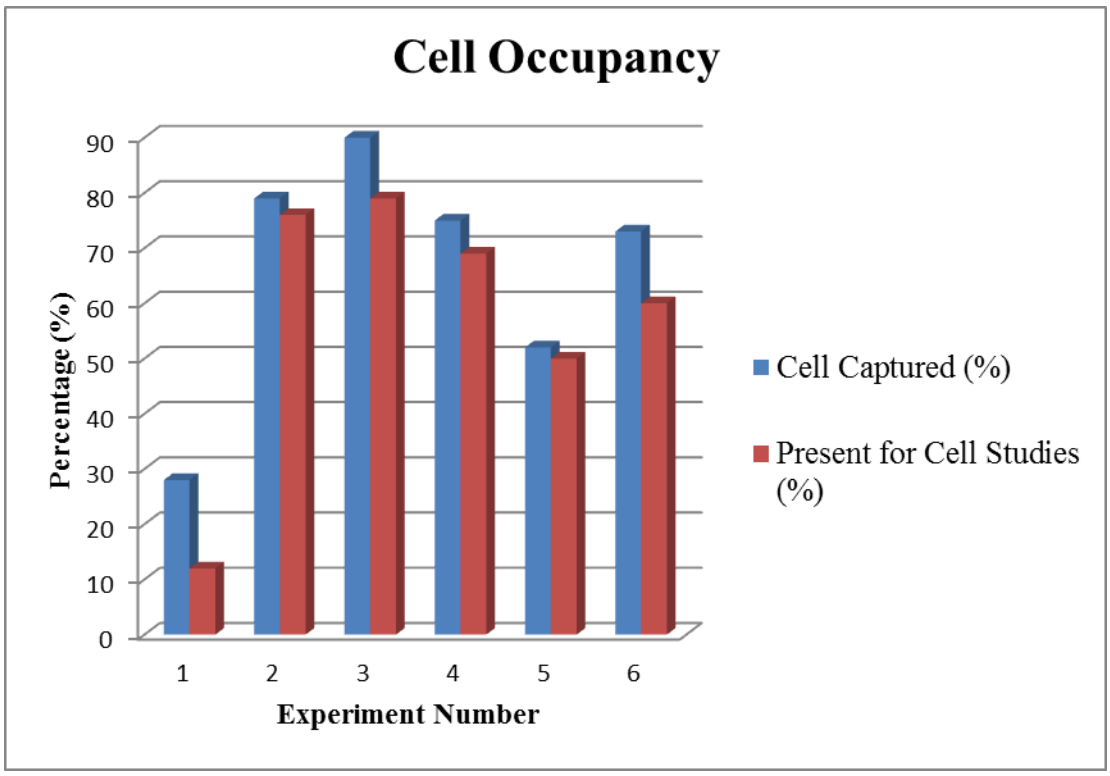

% cells captured = cells trapped during the loading process

% present for cell studies= cells present on the chip once the chip is removed from the cell loader

4.3 Drawdown Experiment Results

The completed microfluidic platform can now be used to measure the OCR (drawdown) of the cells in the wells. The sensor intensity data extracted from the images are defined by Regions of Interest (ROI). The ROI is the region which is around the sensor area which is responding to the sensor change and is used to calculate the average intensity of the sensor area (Kelbauskas et al. 2012). Data

analysis and extraction from the images were performed using a LabVIEW program written to extract the average intensities from the images captured. The average intensity (I_{ave}) was calculated using the following equation:

$$I_{ave} = \frac{\sum_{k=1}^{N} I_k}{N} \qquad [2]$$

The ROIs were generated using the program and the response of the sensor was then plotted in Microsoft Excel.

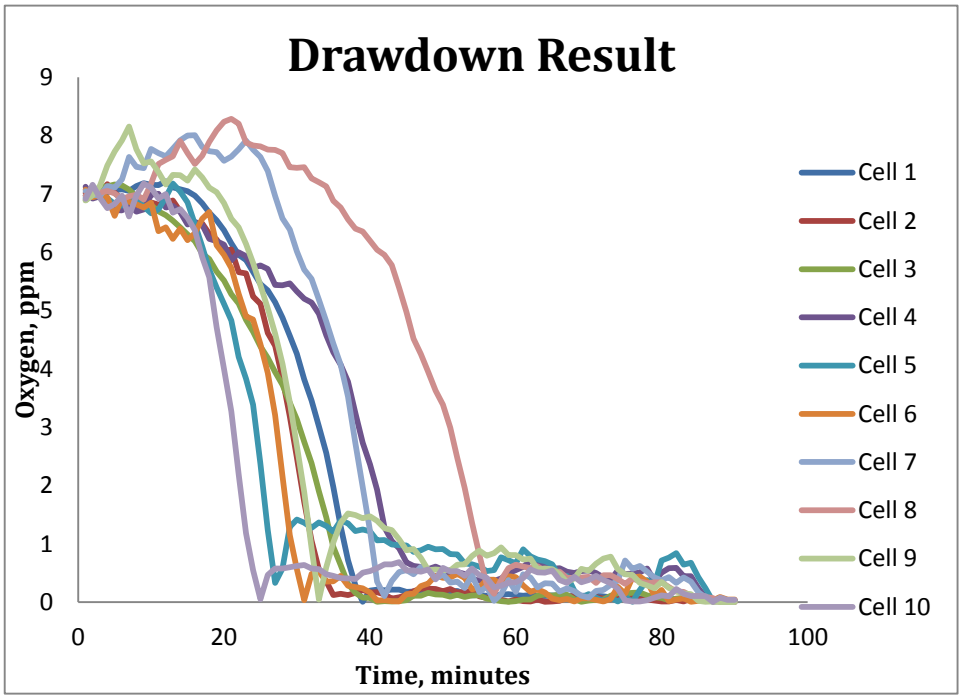

Figure 20: The Graph showing Oxygen Change during a Drawdown Experiment.

Figure 20 shows the OCR's of CP-A cells. All experiments were conducted using the same loading, incubation and OCR measurements conditions. Data obtained from the experiments were then converted into oxygen in ppm, present in each well.

Table 4: Data for Successful Drawdown Experiments.

Experiment Number	Number of wells under observation	Number of responding wells	Exposure time (msec)	LED Intensity (mA)
1	77	45	100	50
2	69	51	100	50
3	69	41	100	50

Table 5: Number of Successful Drawdowns Experiments.

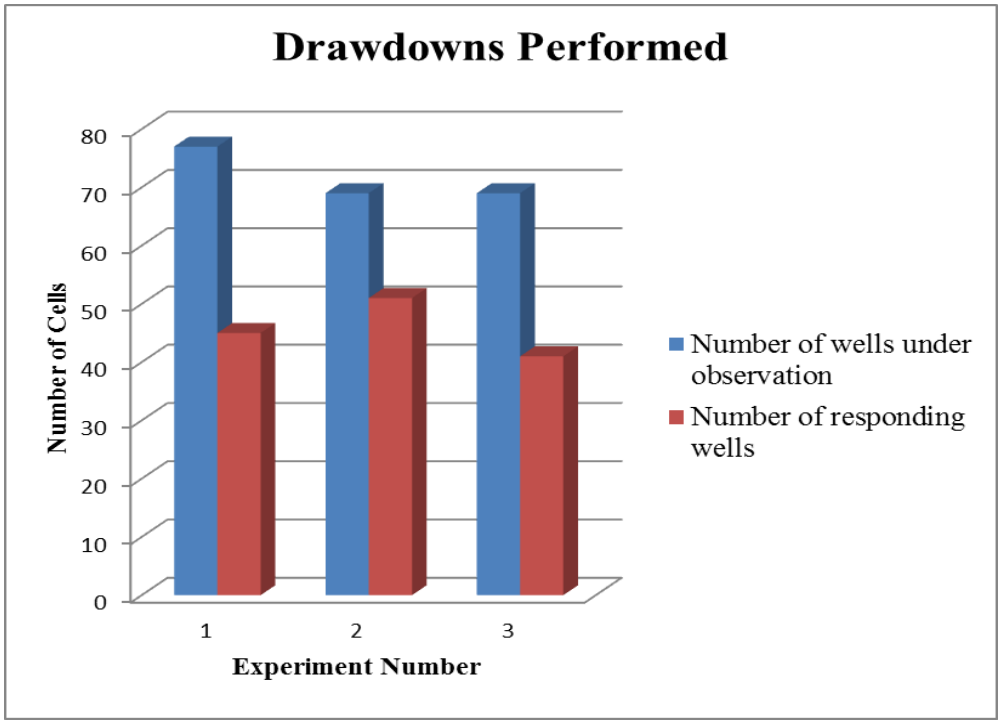

CHAPTER 5: CONCLUSION AND FUTURE OUTLOOK

5.1 Contributions

In this thesis, a device was designed, optimized and implemented to measure the oxygen consumption rate (OCR) of live single cells. A microfluidic device was designed with the ability to rapidly seal and unseal microchambers containing individual cells and an extracellular optical oxygen sensor for measuring the OCR of live single cells. The device consists of two parts, one chip with the sensor in microwells (top half, "sensor chip") and the other chip with channels and cells trapped in Pachinko-type micro-traps (bottom half, "cell chip"). Experiments with the device demonstrate the use of oil as a sealing medium and a proof of principle that a sealed environment can be achieved for live single cell analysis. Oxygen consumption rate results show that the device can be used for analysis of live single cells. It was also demonstrated **(Figure 8)** that the device can further be used to perform tests other than physiological measurements of the cell processes by introducing different biochemical fluids into the device.

5.1.1 Microfluidic Approach

The data presented demonstrates the capability of the fluid (oil) in the device to achieve a seal to perform oxygen consumption rate measurements at the single cell level. The new approach is more advantageous than existing technologies which use glass-on-glass with force for attaining a hermetic seal (Kelbauskas et al. 2012)(Molter et al. 2009). In this thesis, a process was developed to flow oil through the channels to provide a seal around the wells containing the cells. Properties of

mineral oil, such as interfacial forces and the separation factor, were used to successfully design the seal around the cells and to prevent oxygen from the environment to enter into the system.

The introduction of the 2 μm gap between the two closed chips allowed the easy and quick replacement of fluids within the channel and the wells. The diffusion test performed proved this by the replacement of medium within the wells with fresh medium. The whole process takes only a few seconds to wash out all the fluid from the system with fresh fluid, making the device capable of being used for further analysis or successive drawdown experiments. The flexibility of fluid exchange can further be used for performing various other biological studies. For example, physiological measurements could be performed followed by or in conjunction with the introduction of chemical stimuli for drug dose-response studies. The microfluidic device can be used to deliver different biochemical and environmental stimuli to study live single cells within the wells. After live cell metabolic measurements are performed, gene transcription levels could be measured for each single cell and the measurements correlated. The flow rate throughout the system is manually controlled using syringes and tubes.

5.1.2 Cell Loading Mechanism

The flexible design for cell loading allows single cells to be captured within the trap (100 cell traps) achieving nearly 100% occupancy rate in 30-60 seconds. Trapping single cells in each trap helps in performing experiments with a high efficiency of nearly 90-100 cells/drawdown experiment. The experiment used only a single type

of cell line (CP-A) but the scope of the study can further be extended by using other cell lines by loading them into the system for oxygen consumption rate measurements. The use of the microfluidic fixture to load cells has increased the rate at which cells are loaded into the chip.

5.1.3 Sensor Deposition

The sensor was loaded into a separate chip with wells which prevented the cells from coming into close contact with the sensor since they are loaded into a different chip. A dual pH and oxygen ratiometric sensor was used which has the capability of measuring oxygen and pH changes. Experiments measured only the oxygen changes of cells within the wells, but further tests could be performed to measure both the oxygen and pH changes of single cells.

5.2 Future Work

Implementing automated, feedback-controlled syringe pumps which have a controlled flow rate would improve system performance by automating and optimizing the entire process of flowing medium and oil through the system at a required rate to increase efficiency and reproducibility. Taking advantage of the cell loading mechanism, the cell loader can be scaled to have higher numbers of traps and can further be used to load 1,000 to 10,000 cells into chips in just a few minutes giving even higher throughput. The cell loader system uses a manually controlled three-way valve system for the flow rate. Cell loading can be improved by incorporating an automated syringe pump. Optimizing the flow rate for loading the cells can increase the efficiency of the system.

The present sensor deposition method fails to deposit sensor in some of the wells, reducing the efficiency of the system. A better and quicker sensor deposition method could improve the throughput of the device. The thickness of the bottom chip with the wells can be reduced to enable high resolution microscopy. Future work would concentrate on developing a new design having a chip with an array of 1,000 to 10,000 or 100,000 wells and another one with the same number of cell traps within channels to achieve higher throughput.

REFERENCES

Ashili, Shashanka P., Laimonas Kelbauskas, Jeff Houkal, Dean Smith, Yanqing Tian, Cody Youngbull, Haixin Zhu, et al. "Automated Platform for Multiparameter Stimulus Response Studies of Metabolic Activity at the Single-Cell Level," *Proceedings of SPIE*, Edited by Holger Becker and Bonnie L. Gray 7929, no. 480 (February 10, 2011): 79290S–79290S–12. doi:10.1117/12.875438.

Beckman, Robert a, Gunter S Schemmann, and Chen-Hsiang Yeang. "Impact of Genetic Dynamics and Single-Cell Heterogeneity on Development of Nonstandard Personalized Medicine Strategies for Cancer." *Proceedings of the National Academy of Sciences of the United States of America* 109, no. 36 (September 04, 2012): 14586–91. doi:10.1073/pnas.1203559109.

Diepart, Caroline, Julien Verrax, Pedro Buc Calderon, Olivier Feron, Bénédicte F Jordan, and Bernard Gallez. "Comparison of Methods for Measuring Oxygen Consumption in Tumor Cells in Vitro." *Analytical Biochemistry* 396, no. 2 (January 15, 2010): 250–56. doi:10.1016/j.ab.2009.09.029.

Geiler-Samerotte, K a, C R Bauer, S Li, N Ziv, D Gresham, and M L Siegal. "The Details in the Distributions: Why and How to Study Phenotypic Variability." *Current Opinion in Biotechnology* 24, no. 4 (August 2013): 752–59. doi:10.1016/j.copbio.2013.03.010.

Junker, Jan Philipp, and Alexander van Oudenaarden. "Every Cell Is Special: Genome-Wide Studies Add a New Dimension to Single-Cell Biology." *Cell* 157, no. 1 (March 27, 2014): 8–11. doi:10.1016/j.cell.2014.02.010.

Kelbauskas, Laimonas, Shashanka P Ashili, Jeff Houkal, Dean Smith, Aida Mohammadreza, Kristen B Lee, Jessica Forrester, et al. "Method for Physiologic Phenotype Characterization at the Single-Cell Level in Non-Interacting and Interacting Cells." *Journal of Biomedical Optics* 17, no. 3 (March 2012): 037008. doi:10.1117/1.JBO.17.3.037008.

Kuang, Yina, and David R Walt. "Detecting Oxygen Consumption in the Proximity of Saccharomyces Cerevisiae Cells Using Self-Assembled Fluorescent Nanosensors," *Biotechnology and Bioengineering*, Vol. 96, no. 2 (2007): 318–25. doi:10.1002/bit.

Lidstrom, Mary E, and Deirdre R Meldrum. "Life-on-a-Chip," *Nature Reviews Microbiology* 1, no.2, (November 2003): 158–64.

Lindström, Sara, and Helene Andersson-Svahn. "Overview of Single-Cell Analyses: Microdevices and Applications." *Lab on a Chip* 10, no. 24 (December 21, 2010): 3363–72. doi:10.1039/c0lc00150c.

Mannello, Ferdinando, and Daniela Ligi. “Deciphering the Single Cell Omic Innovative Application for Translational Medicine,” *Expert Review of Proteomics*.9.6 (Dec. 2012): p635.

Molter, Timothy W, Sarah C McQuaide, Martin T Suchorolski, Tim J Strovas, Lloyd W Burgess, Deirdre R Meldrum, and Mary E Lidstrom. “A Microwell Array Device Capable of Measuring Single-Cell Oxygen Consumption Rates.” *Sensors and Actuators. B, Chemical* 135, no. 2 (January 15, 2009): 678–86. doi:10.1016/j.snb.2008.10.036.

Piowland, B Y Ruti-i B, and Alan Bernstein. “A method for determining the Oxygen Consumption of a Single Cell,” *The Journal of General Physiology*, pp. 339-348, (1930).

Sarkar, Aniruddh, Sarah Kolitz, Douglas a Lauffenburger, and Jongyoon Han. “Microfluidic Probe for Single-Cell Analysis in Adherent Tissue Culture.” *Nature Communications* 5 (January 2014): 3421. doi:10.1038/ncomms4421.

Tian, Yanqing, Liqiang Zhang, Fengyu Su, Hongguang Lu, Sean Buizer, Kevin Day, Jacob Messner, and Deirdre R Meldrum. “Ratiometric Dual pH and Oxygen Sensors,” *Society for Biomaterials*, no. 5 (2014): 164250.

Zeng, Jia, Jiangxin Wang, Weimin Gao, Aida Mohammadreza, Laimonas Kelbauskas, Weiwen Zhang, Roger H Johnson, and Deirdre R Meldrum. “Quantitative Single-Cell Gene Expression Measurements of Multiple Genes in Response to Hypoxia Treatment.” *Analytical and Bioanalytical Chemistry* 401, no. 1 (July 2011): 3–13. doi:10.1007/s00216-011-5084-2.

Zettlemoyer, a.C, M.P Aronson, and J.a Lavelle. “Spreading at the Teflon / Oil / Water / Air Interfaces.” *Journal of Colloid and Interface Science* 34, no. 4 (December 1970): 545–48. doi:10.1016/0021-9797(70)90217-1.